

Leading twist moments of the neutron structure function F_2^n

M. Osipenko^{1,2}, W. Melnitchouk³, S. Simula⁴, S. Kulagin⁵,
G. Ricco^{1,6}

¹Istituto Nazionale di Fisica Nucleare, Sezione di Genova, 16146 Genova, Italy

²Skobeltsyn Institute of Nuclear Physics, 119992 Moscow, Russia

³Jefferson Lab, Newport News, Virginia 23606, USA

⁴Istituto Nazionale di Fisica Nucleare, Sezione Roma III, 00146 Roma, Italy

⁵Institute for Nuclear Research of Russian Academy of Science, 117312 Moscow, Russia

⁶Dipartimento di Fisica dell'Università di Genova, 16146 Genova, Italy

Abstract

We perform a global analysis of neutron F_2^n structure function data, obtained by combining proton and deuteron measurements over a large range of kinematics. From these data the lowest moments ($n \leq 10$) of the leading twist neutron F_2^n structure function are extracted. Particular attention is paid to nuclear effects in the deuteron, which become increasingly important for the higher moments. Our results for the nonsinglet, isovector $p - n$ combination of the leading twist moments are compared with those of available lattice simulations. We also determine the lowest few moments of the higher twist contributions, obtained by subtracting the leading twist from the total structure function, and analyze their isospin dependence.

1 Introduction

Inclusive lepton scattering experiments have for some time been the standard tool with which to study the internal quark-gluon structure of nucleons and nuclei. In unpolarized scattering, this structure is represented through two structure functions, F_1 and F_2 , which parameterize the differential cross section,

$$\frac{d^2\sigma}{d\Omega dE'} = \sigma_{\text{Mott}} \left[\frac{2F_1(x, Q^2)}{M} \tan^2 \frac{\theta}{2} + \frac{F_2(x, Q^2)}{\nu} \right], \quad (1)$$

where $\sigma_{\text{Mott}} = (4\alpha^2 E'^2/Q^4) \cos^2 \frac{\theta}{2}$ is the Mott cross section for the scattering from point particles, with Ω the scattered lepton solid angle (θ is the polar scattering angle), and E' the recoil lepton energy. Here ν is the energy transfer and M is the nucleon mass. The structure functions $F_{1,2}$ are functions of the four-momentum transfer squared $q^2 \equiv -Q^2$, and the Bjorken scaling variable $x = Q^2/2M\nu$. In the Bjorken limit ($Q^2, \nu \rightarrow \infty$, x fixed), the structure functions can be related to parton distribution functions, which give the light-cone momentum distributions of quarks (and gluons, or partons in general) in the hadron. At leading order, one has $F_2 = 2xF_1 = x \sum_i e_i^2 (q_i(x, Q^2) + \bar{q}_i(x, Q^2))$. At finite Q^2 radiative corrections and higher twist effects give rise to a Q^2 dependence in the structure functions, leading to scaling violations.

The connection between the partonic structure of hadrons and QCD can be most readily made through *moments*, or x -weighted integrals, of structure functions, which through the operator product expansion (OPE) can be related to hadronic matrix elements of local operators. In the case of the F_2 structure function, to which we restrict ourselves in the following, the moment is defined by

$$M_n(Q^2) = \int_0^1 dx x^{n-2} F_2(x, Q^2). \quad (2)$$

While in the Bjorken limit the moments are given by real numbers, independent of Q^2 , at finite Q^2 the renormalization group equations lead to a specific Q^2 dependence of the moments that can be calculated from perturbative QCD. In fact, observation of this Q^2 dependence was instrumental in establishing QCD as the theory of the strong nuclear interactions. The moments can also be calculated nonperturbatively using lattice QCD techniques.

A wealth of information has been accumulated over several decades on the structure of the proton, deuteron, as well as heavier nuclei. To completely describe the structure of the nucleon, however, requires knowledge of both the proton *and* neutron structure functions. Typically, the neutron structure function is obtained by combining data on the deuteron and proton. In most analyses the deuteron structure function is assumed to be given by a simple sum of free proton and neutron structure functions, $F_2^D \rightarrow F_2^p + F_2^n$, which is a good approximation for some regions of kinematics ($0.1 \lesssim x \lesssim 0.4$). However, it is well known that at small x ($x \lesssim 0.1$) nuclear shadowing reduces the deuteron structure function relative to the free nucleon [1, 2, 3, 4], while at large x ($x \gtrsim 0.4$)

nuclear binding and Fermi motion corrections are expected to give rise to a small “nuclear EMC effect” in the deuteron.

In terms of moments, any nuclear effect at large x will manifest itself in high moments (large n). It is crucial, therefore, that a moment analysis of the neutron structure function includes a careful treatment of nuclear corrections. In this paper we for the first time perform such an analysis, utilizing the recent high-precision data from Jefferson Lab [5, 6] together with earlier data on F_2^p and F_2^D . Unlike previous studies, which have focussed on the x dependence, and have ignored or underestimated the nuclear corrections, we extract the lowest few moments of the neutron F_2^n taking into account the systematic uncertainties associated with our knowledge of nuclear effects in the deuteron. Furthermore, this analysis directly uses the leading twist parts of the moments extracted from the F_2^p and F_2^D data, which allows a more straightforward implementation of the impulse approximation.

The general framework for analyzing the data is presented in Sec. 2, where we discuss various models of nucleon light-cone momentum distributions in the deuteron. The extracted leading twist neutron moments are presented in Sec. 3, where we also discuss corrections to the simple one-dimensional convolution formalism, in the form of nucleon off-shell effects, as well as nuclear shadowing and meson exchange currents. The results for the extracted moments are compared with those obtained from several global parton distribution functions. Moreover we construct the nonsinglet, isovector $p - n$ combination of the leading twist moments and compare our results with available lattice ones. As an interesting application of our extraction, in Sec. 4 we identify the isospin dependence of the higher twist contributions to the moments, and speculate about possible interpretations of our findings within a diquark picture. Finally, in Sec. 5 we summarize our results and briefly outline some future directions.

2 Neutron structure and nuclear effects in the deuteron

In the absence of free neutron targets, information on the structure function of the neutron is typically extracted from measurements using deuterons, together with knowledge of the corresponding proton structure function. Since the deuteron is a nucleus, its nucleon constituents are bound, albeit weakly, and in general the structure of the bound nucleons will differ from the free nucleon structure. In this section we describe the various nuclear corrections which enter in the extraction of the free neutron F_2 structure function, and in particular its moments, from the structure function of the deuteron.

We begin with the standard nuclear impulse approximation, in which the virtual photon scatters incoherently from individual nucleons in the deuteron, and discuss several implementations of the convolution formula. Following this we describe corrections to convolution, associated with nucleon off-shell effects, nuclear shadowing, and meson exchange currents.

2.1 Impulse approximation

For moderate to large values of x ($x \gtrsim 0.1$) inclusive scattering off a deuteron can be described, using the optical theorem, in terms of the amplitudes $\gamma^*N^* \rightarrow \gamma^*N^*$ and $N^*d \rightarrow N^*d$, where N^* refers to the fact that the nucleon is off its mass or energy shell. In this approximation interactions between the intermediate states of the γ^*N^* and N^*d subprocesses are neglected. Formally, the deuteron F_2 structure function can then be written as

$$F_2^D(x, Q^2) = \int d^4p \text{Tr} \left[\widehat{\mathcal{W}}(p, q) \cdot \widehat{\mathcal{A}}(p, p_D) \right], \quad (3)$$

where p , p_D and q are the virtual nucleon, deuteron and virtual photon four-momenta, respectively, the Dirac matrix $\widehat{\mathcal{W}}(p, q) = I \mathcal{W}_0 + \not{p} \mathcal{W}_1 + \not{q} \mathcal{W}_2$ is the truncated (off-shell) nucleon structure function, and $\widehat{\mathcal{A}}(p, p_D) = I \mathcal{A}_0 + \gamma_\alpha \mathcal{A}_1^\alpha$ is the off-shell nucleon–deuteron scattering amplitude. The amplitudes \mathcal{A}_0 and \mathcal{A}_1^α depend on the deuteron wave functions.

For an on-shell nucleon, the F_2 structure function is proportional to $M \mathcal{W}_0 + M^2 \mathcal{W}_1 + p \cdot q \mathcal{W}_2$. In general the presence of several Dirac structures and corresponding “structure functions” \mathcal{W}_i in the trace in the integrand in Eq. (3) complicates the relation between the deuteron and nucleon structure functions. There are various ways which the formal expression in Eq. (3) can be simplified, however, as we now discuss.

2.1.1 Nonrelativistic expansion

The formal expression for the deuteron structure function F_2^D in Eq. (3) is Lorentz-invariant and can be evaluated in any reference frame. Without loss of generality, however, one can choose to work in the deuteron rest frame, and take the z -axis such that $q_z = -|\mathbf{q}|$. Performing a nonrelativistic reduction of the Dirac traces in Eq. (3), one can show that to order \mathbf{p}^2/M^2 in the Bjorken limit the product of the Dirac structures reduces to a single structure proportional to a generalized (off-shell) nucleon structure function [4],

$$F_2^D(x, Q^2) = \int \frac{d^3\mathbf{p}}{(2\pi)^3} \left(1 + \frac{p_z}{M}\right) |\Psi_D(\mathbf{p})|^2 F_2^N\left(\frac{x}{z}, Q^2, p^2\right). \quad (4)$$

Here $F_2^N = \frac{1}{2}(F_2^p + F_2^n)$ is the isoscalar nucleon structure function, $z = (p_0 + p_z)/M$ is the light-cone momentum fraction of the deuteron carried by the interacting nucleon, where $p_0 = M + \varepsilon_D - \mathbf{p}^2/(2M)$ is the energy of the struck nucleon, and $\varepsilon_D = -2.22$ MeV is the deuteron binding energy. The deuteron wave function Ψ_D contains the usual nonrelativistic S - and D -wave components, ψ_0 and ψ_2 ,

$$\frac{1}{2\pi^2} |\Psi_D(\mathbf{p})|^2 = \psi_0^2(|\mathbf{p}|) + \psi_2^2(|\mathbf{p}|), \quad (5)$$

normalized such that

$$\int_0^\infty d|\mathbf{p}| \mathbf{p}^2 |\Psi_D(\mathbf{p})|^2 = 1. \quad (6)$$

Note that in addition to the Bjorken variable and Q^2 , the nucleon structure function in (4) also depends on the nucleon off-shellness $p^2 \equiv p_0^2 - \mathbf{p}^2$. If one neglects the dependence of F_2^N on p^2 , then Eq. (4) leads to the simple one-dimensional convolution formula in terms of the free nucleon structure function [7, 8],

$$F_2^{D(\text{conv})}(x, Q^2) = \int_x^{M_D/M} dz f_{\text{nr}}^D(z) F_2^N\left(\frac{x}{z}, Q^2\right), \quad (7)$$

where M_D is the deuteron mass, and $f_{\text{nr}}^D(z)$ is the nonrelativistic nucleon (light-cone) momentum distribution in the deuteron,

$$f_{\text{nr}}^D(z) = \int \frac{d^3\mathbf{p}}{(2\pi)^3} \left(1 + \frac{p_z}{M}\right) |\Psi_D(\mathbf{p})|^2 \delta\left(z - \frac{p_0 + p_z}{M}\right). \quad (8)$$

Physically the function $f_{\text{nr}}^D(z)$ describes the Fermi motion and binding of nucleons in the deuteron. Note that some implementations of the convolution formula (7) do not include the ‘‘flux factor’’ $(1 + p_z/M)$ [9]. However, since this appears at $\mathcal{O}(\mathbf{p}/M)$, consistency to order \mathbf{p}^2/M^2 requires its inclusion [4]. The wave function normalization (6) ensures that

$$\int_0^{M_D/M} dz f_{\text{nr}}^D(z) = 1, \quad (9)$$

which guarantees that (for the valence component) the convolution term alone preserves the baryon number of the deuteron.

2.1.2 Relativistic effects

Because the deuteron is a weakly bound nucleus, in most calculations of deuteron structure the nonrelativistic approximation is adequate. In the large- x region, however, one is more sensitive to the large-momentum components of the deuteron wave function. In this case relativistic effects are expected to become more important.

Since the distribution function f_{nr}^D in Eq. (8) was obtained in the nonrelativistic approximation, it applies in the region $|z - 1| \ll 1$. Outside of this region relativistic corrections may be important. In order to test the sensitivity to these effects we also consider a relativistic version of the distribution in Eq. (8) which is calculated with the same nonrelativistic wave function but using relativistic kinematics, namely $p_0 = M_D - E_p$, where $E_p = \sqrt{M^2 + \mathbf{p}^2}$ is the energy of the spectator nucleon. Furthermore, one also replaces the ratio p_z/M in the flux factor with p_z/E_p .

While most deuteron wave functions calculated to date have been nonrelativistic, there have been some models which have treated the two-nucleon system relativistically [10, 11, 12]. In order to consistently utilize the relativistic wave functions, one needs to work with the full expression for the structure function in Eq. (3) directly. This necessarily involves modeling the off-shell nucleon structure functions, which introduces additional model dependence in the calculation [13].

One can show, however, that the exact expression in Eq. (3) can be reduced to an on-shell convolution part, similar to that in Eq. (7), plus nuclear off-shell and relativistic corrections [14, 15],

$$F_2^D(x, Q^2) = F_2^{D(\text{conv})}(x, Q^2) + \delta^{(\text{off})} F_2^D(x, Q^2) . \quad (10)$$

The convolution component here now involves a relativistic nucleon light-cone distribution function [14],

$$f_{\text{rel}}^D(z) = zM_D \int_{-\infty}^{p_{\text{max}}} \frac{dp^2}{16\pi^2} \frac{E_p}{p_0} |\tilde{\Psi}_D(\mathbf{p})|^2 , \quad (11)$$

where $E_p = \sqrt{M^2 + \mathbf{p}^2} = (M^2 - p^2 + M_D^2)/2M_D$ is the energy of the (on-shell) nucleon spectator, and the upper limit of the nucleon virtuality p^2 in the integration is given by $p_{\text{max}}^2 = zM_D^2/2 - zM^2/(2 - z)$. In addition to the usual S - and D -state wave functions u and w , the wave function $\tilde{\Psi}_D(\mathbf{p})$ also includes the relativistic P -states [11, 12]

$$\frac{1}{2\pi^2} |\tilde{\Psi}_D(\mathbf{p})|^2 = \psi_0^2(|\mathbf{p}|) + \psi_2^2(|\mathbf{p}|) + \psi_{1t}^2(|\mathbf{p}|) + \psi_{1s}^2(|\mathbf{p}|) , \quad (12)$$

where ψ_{1s} and ψ_{1t} correspond to the singlet and triplet P -states, respectively. Note that the function f_{rel}^D also includes the relativistic flux factor, $(E_p/p_0) z$ [9], and therefore satisfies the same normalization condition as in Eq. (9), $\int dz f_{\text{rel}}^D = 1$. One should point out, however, that the separation of F_2^D into the two terms in Eq. (10) is not unique (the sum, of course, is unique). However, the choice (11) is the most natural one, and corresponds to that which has been followed in many phenomenological treatments.

2.1.3 Light-cone formulation

An alternative to the covariant (instant-form) formulations of scattering from the deuteron is the Hamiltonian light-cone (LC) approach. Here the intermediate state nucleons are on-mass-shell, but off-energy-shell, so that one avoids the explicit p^2 dependence in the bound nucleon structure function in Eq. (4).

Because the nucleons are on-mass-shell, the derivation of the one-dimensional convolution from Eq. (3) is trivial since each of the three terms in the trace factor become proportional [13]. The LC nucleon momentum distribution in the deuteron is given by [16]

$$f_{\text{LC}}^D(z) = \int_{|\mathbf{p}|_{\text{min}}} d|\mathbf{p}| |\mathbf{p}| \sqrt{M^2 + \mathbf{p}^2} |\Psi_D^{\text{LC}}(\mathbf{p})|^2 , \quad (13)$$

where $|\mathbf{p}|_{\text{min}} = M|z - 1|/\sqrt{z(2 - z)}$, and Ψ_D^{LC} is the LC deuteron wave function. Since most of the two-nucleon phenomenology has traditionally been formulated within the instant-form approach, in practice for Ψ_D^{LC} one has usually employed the S - and D -state wave functions as calculated in nonrelativistic potential models [see Eq. (5)].

Note that in the limit where the nucleons are free (i.e. not bound), the deuteron can be described in terms of an NN Fock state component. Inclusion of binding requires the addition of NN +meson Fock states. Technically, binding or off-shell effects in the LC

approach can be included by constructing a wave function which explicitly depends on an additional light-like four-vector related to the orientation of the null-plane [17]. This introduces a number of additional wave functions, which would need to be included in f_{LC}^D . Recently calculations of deuteron LC wave functions have been performed within this framework, and some of the additional wave functions found to be important at large momentum. While it is interesting to explore the phenomenology using these wave functions, in the present study we shall compare the results of the LC distribution f_{LC}^D using the nonrelativistic S - and D -state wave functions as used in the literature.

In the next section we compare the various light-cone momentum distributions discussed above, for different model deuteron wave function models.

2.2 Nucleon momentum distributions

Within the convolution approximation there are two sources of nuclear model dependence in the calculation of the deuteron structure function. Firstly, as discussed above, different approaches are used to formulate scattering from the two-nucleon system – nonrelativistic, relativistic, or light-cone. In addition, within each approach there is dependence on the deuteron wave function or NN potential. It is beyond the scope of this work to critically analyze the merits of the various models; instead we survey a reasonably large sample of models and estimate the systematic uncertainty from the spread in their predictions.

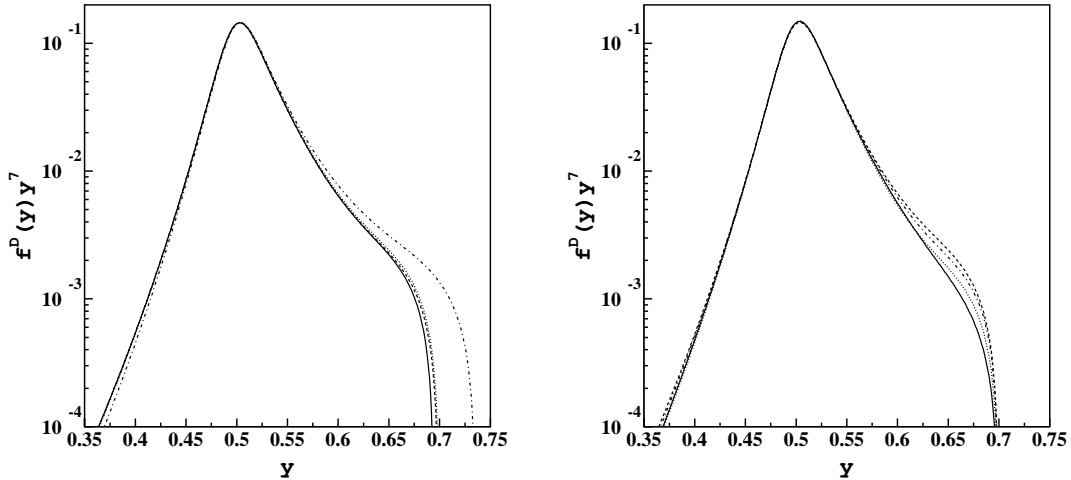


Figure 1: Nucleon light-cone momentum distribution f^D weighted by y^7 , where $y = z/2$, for various models: (a) nonrelativistic distribution (8) (solid), distribution (8) with relativistic kinematics (dashed), relativistic model (11) (dotted), light-cone distribution (13), all using the Paris wave function [18]; (b) relativistic distribution (11) using the Bonn [19] (solid), Paris [18] (dashed), and relativistic Gross wave functions from Refs. [11] (dotted) and [12] (dot-dashed).

In practice the deuteron wave functions are determined by fitting NN scattering data. Since most of the data are at low momentum, the wave functions are relatively well constrained at small p , but the large- p tail of the wave function is more model dependent. In terms of the light-cone variable z , the large- p region corresponds to large values of z . To emphasize the large- z region of f^D we plot in Fig. 1 the various nucleon momentum distributions, for different wave functions, weighted by y^7 , where $y \equiv z/2$. Note that the momentum integration in each of the curves has been limited to $|\mathbf{p}| = 0.5$ GeV (see below). As expected the model dependence is relatively weak for moderate z , and only becomes significant for $z \gtrsim 0.6 - 0.7$.

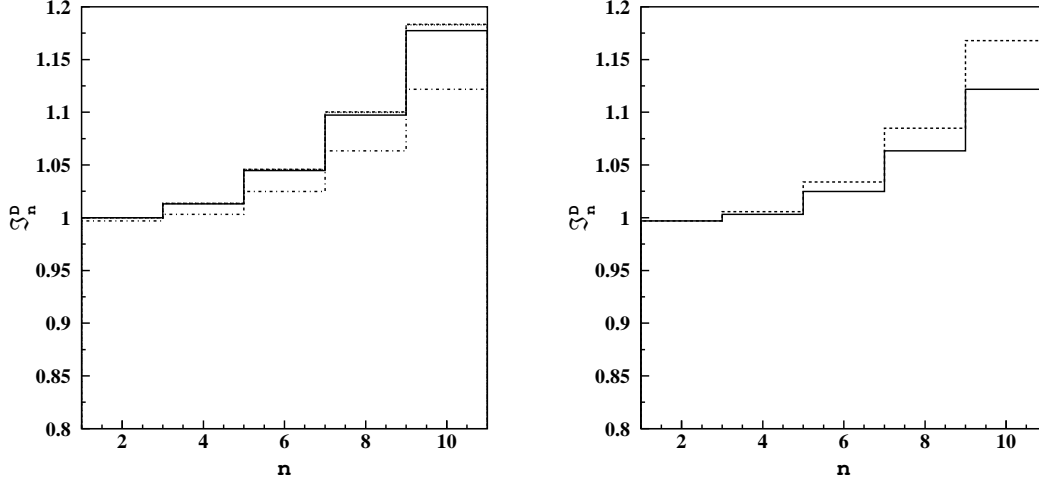


Figure 2: Moments \mathcal{F}_n^D ($n = 2 - 10$) of the nucleon light-cone momentum distribution $f^D(z)$ in Eq. (11) (a) for different deuteron wave functions: BonnCD [20] (solid), Nijmegen 93 [21] (dashed), Argonne v_{18} [22] (dotted), Gross [11] (dot-dashed); (b) for the Gross wave function [12] with the momentum integration restricted to $p_{\max} = 0.5$ GeV (solid) and 1 GeV (dashed).

Uncertainties due to the nuclear models can also be quantified in terms of moments. This is actually more relevant for the present analysis since ultimately we extract the moments of the neutron F_2^n structure function. If we define the n -th moment of the distribution $f^D(z)$ by

$$\mathcal{F}_n^D = \int_0^{M_D/M} dz z^{n-1} f^D(z), \quad (14)$$

then clearly the uncertainties in the large- z part of the distribution will be reflected in the uncertainties of the moments of f^D at large- n , which are illustrated in Fig. 2.

As mentioned above, the differences between the momentum distributions at large z arise because the deuteron wave function is not well constrained at large momentum. In fact, NN scattering data which have been used to constrain the deuteron wave function typically extend only to $p \approx 0.4$ GeV. At large momentum ($p \gtrsim 0.3 - 0.4$ GeV) the

inter-nucleon distances probed becomes smaller than the nucleon radius, so that here a description in terms of nucleon degrees of freedom alone may be questionable. To estimate the uncertainty arising from the large- p tail of the deuteron wave function, we examine the effect of truncating the momentum integration at $p = p_{\max}$. The moments \mathcal{F}_n^D of the distribution $f^D(z)$ with $p_{\max} = 0.5$ and 1 GeV are plotted in Fig. 2(b), where the distributions have been renormalized to satisfy Eq. (9). For low moments ($n = 2, 4$) the effect is negligible, while for the $n = 10$ moment the effect of the $p_{\max} = 0.5$ (1) GeV cuts is 6% (1%). We estimate that the uncertainty introduced by our poor knowledge of the large- p components of the deuteron wave function is of the same order of magnitude as the wave function model dependence. The maximum deviation among the moments obtained with different deuteron wave functions will be taken as an estimate of the systematic error due to the wave function model dependence.

An independent test of the nucleon distribution functions may be made by considering quasi-elastic scattering. Within the impulse approximation and neglecting finite- Q^2 effects, the quasi-elastic contribution to the deuteron structure function, $F_2^{D(QE)}$, can be written in factorized form, in terms of the nucleon distribution function f^D and the nucleon elastic form factors,

$$F_2^{D(QE)}(x_D, Q^2) \rightarrow \frac{1}{2} x_D f^D(x_D) \left\{ \frac{G_E^{p,2}(Q^2) + G_E^{n,2}(Q^2) + \tau(G_M^{p,2}(Q^2) + G_M^{n,2}(Q^2))}{1 + \tau} \right\}, \quad (15)$$

where $x_D \equiv Q^2/2M_D\nu \simeq x/2$. Thus, one can define *phenomenological* nucleon distribution moments $\tilde{\mathcal{F}}_n^D(Q^2)$ in terms of the moments $M_n^{D(QE)}(Q^2)$ of the deuteron quasi-elastic structure function $F_2^{D(QE)}$ and the nucleon form factors,

$$\tilde{\mathcal{F}}_n^D(Q^2) = \frac{(1 + \tau)M_n^{D(QE)}(Q^2)}{G_E^{p,2}(Q^2) + G_E^{n,2}(Q^2) + \tau(G_M^{p,2}(Q^2) + G_M^{n,2}(Q^2))}. \quad (16)$$

We expect that $\tilde{\mathcal{F}}_n^D(Q^2) \simeq \mathcal{F}_n^D$ at large enough Q^2 . Note that for the moment $M_n^{D(QE)}(Q^2)$ we use the Nachtmann definition [23] to eliminate the finite- Q^2 effects due to the nonzero target mass (i.e. the deuteron mass),

$$M_n^{D(QE)}(Q^2) \rightarrow \int_0^1 dx_D \frac{\xi_D^{n+1}}{x_D^3} F_2^{D(QE)}(x_D, Q^2) \frac{3 + 3(n+1)r_D + n(n+2)r_D^2}{(n+2)(n+3)}, \quad (17)$$

where $r_D = \sqrt{1 + 4M_D^2 x_D^2 / Q^2}$ and $\xi_D = 2x_D / (1 + r_D)$.

The deuteron quasi-elastic contribution to the structure function $F_2^{D(QE)}$ has been calculated using the approach developed in Ref. [24], which includes final state interactions and has been tested against the recent deuteron experimental data of Ref. [6]. As an illustration, the extracted $\tilde{\mathcal{F}}_2^D(Q^2)$ and $\tilde{\mathcal{F}}_6^D(Q^2)$ moments are shown in Fig. 3 as a function of Q^2 , and compared with the corresponding moments \mathcal{F}_2^D and \mathcal{F}_6^D calculated from the distribution function $f^D(z)$ in Eq. (14). The results agree well within the nuclear model uncertainties.

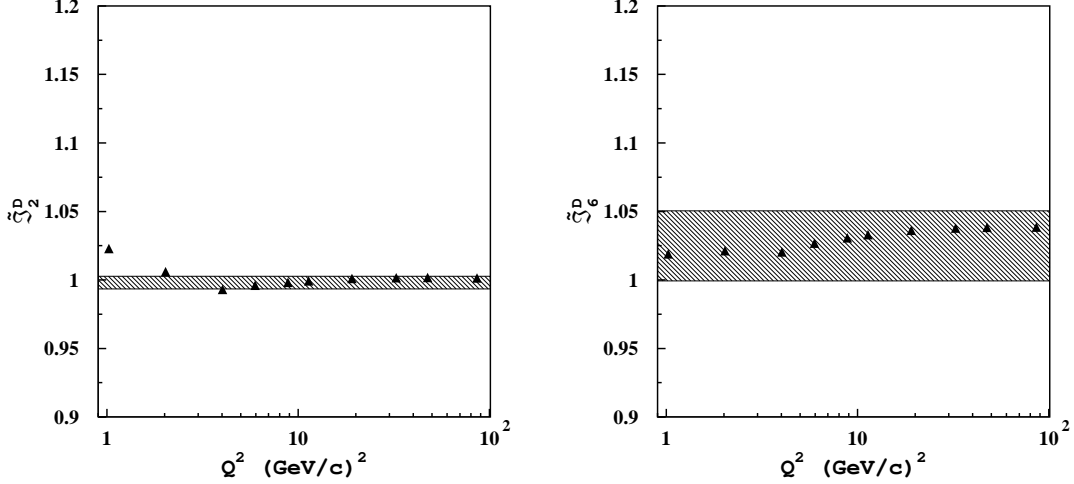


Figure 3: Moments $\tilde{\mathcal{F}}_2^D(Q^2)$ (a) and $\tilde{\mathcal{F}}_6^D(Q^2)$ (b) extracted from the quasi-elastic peak moments defined in Eq. (16) (triangles). The hatched areas represent the corresponding moments \mathcal{F}_2^D and \mathcal{F}_6^D calculated from Eq. (14), including the nuclear model uncertainties shown in Fig. 2.

2.3 Off-shell effects

The expressions for the deuteron structure function thus far have been in the framework of the one-dimensional convolution formula, in which nucleon off-shell, relativistic, and other effects beyond the impulse approximation are neglected. While this constitutes a reasonable approximation at moderate x , or for low moments, at large (and very small) x values these effects will become more important.

Within the nonrelativistic approach discussed in Sec. 2.1.1, the fact that the structure of bound nucleons can differ from that of free nucleons is incorporated in the dependence of the bound nucleon structure function in Eq. (4) on the nucleon virtuality, or off-shellness, p^2 . Since the deuteron is treated as a nonrelativistic system, the off-shellness parameter $v \equiv (p^2 - M^2)/M^2$ is on average a small number. Expanding the leading twist structure function in v and keeping only the first order correction in v , one finds

$$F_2^N(x, Q^2, p^2) = F_2^N(x, Q^2) (1 + \delta f_2(x) v) , \quad (18)$$

$$\delta f_2 = \partial \ln F_2^N / \partial \ln p^2 , \quad (19)$$

where the first term on the right in Eq. (18) is the structure function of the on-mass-shell nucleon, and the derivative is evaluated at $p^2 = M^2$. The deuteron structure function F_2^D can then be written as in Eq. (10), with

$$\delta^{(\text{off})} F_2^D(x, Q^2) = \int \frac{d^3 \mathbf{p}}{(2\pi)^3} \left(1 + \frac{p_z}{M}\right) |\Psi_D(\mathbf{p})|^2 \delta f_2(x/z, Q^2) v F_2^N(x/z, Q^2) . \quad (20)$$

The off-shell correction δf_2 was studied phenomenologically in Ref. [25] by analyzing data on the ratios of structure functions of different nuclei (EMC ratios). It was found that to a good approximation δf_2 was independent of Q^2 , and could be parameterized as

$$\delta f_2 = C_N(x - x_1)(x - x_0)(1 + x_0 - x) , \quad (21)$$

with the best fit parameters $C_N = 8.1 \pm 0.3$, $x_1 = 0.05$, and $x_0 = 0.448 \pm 0.005$. Furthermore, the off-shell correction to the structure function F_3 is given by the same function δf_2 , which is consistent with the normalization of nuclear valence quark distribution (for more details see Ref. [25]).

Expressing the off-shell correction to F_2^D in terms of moments, one can change the order of the \mathbf{p} and x integrations to obtain

$$M_n^D(Q^2) = \mathcal{F}_n^D M_n^N(Q^2) + \delta C_n \delta M_n^N(Q^2) , \quad (22)$$

where the first term on the right hand side is the usual convolution term and the second is the off-shell correction, with

$$\delta C_n = \int \frac{d^3 \mathbf{p}}{(2\pi)^3} \left(1 + \frac{p_z}{M}\right) z^{n-1} v |\Psi_D(\mathbf{p})|^2 \quad (23)$$

and

$$\delta M_n^N(Q^2) = \int_0^1 dx x^{n-2} \delta f_2(x) F_2^N(x, Q^2) . \quad (24)$$

Writing the nucleon moment in terms of the proton and neutron moments explicitly, $M_n^N = (M_n^p + M_n^n)/2$, one can solve Eq. (22) to express the neutron moment in terms of the experimental proton and deuteron moments, and the theoretical \mathcal{F}_n^D and off-shell corrections,

$$M_n^n(Q^2) = 2M_n^D(Q^2) \left(\frac{1 - \Delta_n^{(\text{off})}}{\mathcal{F}_n^D} \right) - M_n^p(Q^2) , \quad (25)$$

where the off-shell ratio $\Delta_n^{(\text{off})}$ is given by

$$\Delta_n^{(\text{off})}(Q^2) = \frac{1}{M_n^D} \int dx x^{n-2} \delta^{(\text{off})}(x) F_2^D(x, Q^2) , \quad (26)$$

and $\delta^{(\text{off})}$ is defined as

$$\delta^{(\text{off})}(x, Q^2) = \frac{\delta^{(\text{off})} F_2^D(x, Q^2)}{F_2^D(x, Q^2)} . \quad (27)$$

From Eqs. (20), (23) and (24) one can also write the moment correction as

$$\Delta_n^{(\text{off})}(Q^2) = \frac{\delta C_n \delta M_n^N}{2M_n^D} . \quad (28)$$

For the relativistic model of Sec. 2.1.2, the off-shell correction $\delta^{(\text{off})} F_2^D$ receives two contributions: one which depends on the relativistic P -state wave functions ψ_{1s} and ψ_{1t} ,

and one which is given by the off-shell part of the truncated nucleon structure functions $\mathcal{W}_{0,1,2}$. The former was found to be of the order 1% and negative over the whole x range, while the latter was somewhat smaller in magnitude. The total off-shell ratio $\delta^{(\text{off})}$ was parameterized at $Q^2 \approx 5 \text{ GeV}^2$ as [14]

$$\delta^{(\text{off})}(x, Q^2) = a_0(1 + a_1 x^{a_2})(1 - (a_3 - x^{a_4})^{a_5}) , \quad (29)$$

with the parameters $a_0 = -0.014$, $a_1 = 3.0$, $a_2 = 20.0$, $a_3 = 1.067$, $a_4 = 1.5$, and $a_5 = 18.0$. The Q^2 dependence of this ratio was found to be weak. Note that the estimate of $\delta^{(\text{off})}$ in Ref. [14] was based on the set of wave functions in Ref. [11] derived from an NN potential with a pseudoscalar πNN coupling, which are known to give larger P -state contributions than more modern treatments [10, 12]. The correction $\delta^{(\text{off})}$ in Eq. (29) should therefore serve as an upper limit on the size of the off-shell correction in this model.

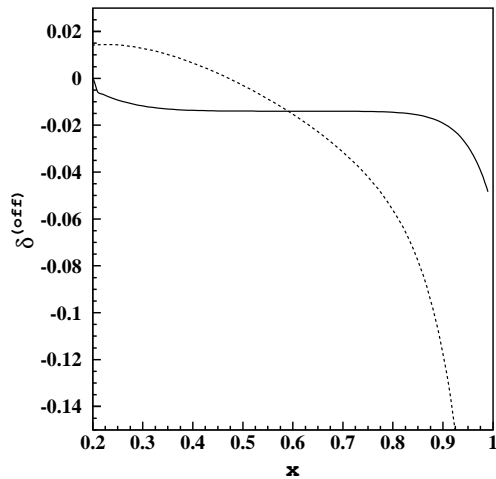


Figure 4: Nucleon off-shell correction $\delta^{(\text{off})}(x, Q^2)$ as a function of x at $Q^2 = 10 \text{ GeV}^2$, in the nonrelativistic [25] (dashed) and relativistic [14] (solid) models.

The x dependence of the corrections $\delta^{(\text{off})}$ in the models of Refs. [14, 25], evaluated using the leading twist parameterization [6] of F_2^D at $Q^2 = 10 \text{ GeV}^2$, is displayed in Fig. 4. Both of the corrections are around 1–2% for $x \lesssim 0.6 - 0.7$, but increase significantly in magnitude for $x \gtrsim 0.8$. The correction at large x is negative in both cases, and is especially dramatic for the model of Ref. [25]. The resulting moments $\Delta_n^{(\text{off})}$ are listed in Table 1 for $n = 2 - 10$. The magnitude of the correction for the lowest moment is similar in the two models, but is of opposite sign. For higher n , the relative importance of the off-shell correction increases. Because of the steep decrease of $\delta^{(\text{off})}$ in the nonrelativistic model [25], the magnitude of the correction $\Delta_n^{(\text{off})}$ at $n = 10$ is about 2-3 times larger than the one in the model of Ref. [14].

Table 1: Moments of the non-convolution corrections to the deuteron F_2^D structure function for $n = 2 - 10$: the first two columns give off-shell corrections $\Delta_n^{(\text{off})}$ in the relativistic [14] and nonrelativistic [25] models, respectively; the third and fourth columns represent the contributions from meson exchange currents and nuclear shadowing [3], respectively.

n	$\Delta_n^{(\text{off})}$ [14]	$\Delta_n^{(\text{off})}$ [25]	$\Delta_n^{(\text{MEC})}$ [3]	$\Delta_n^{(\text{shad})}$ [3]
2	-5.67×10^{-3}	5.08×10^{-3}	2.6×10^{-4}	-1.0×10^{-4}
4	-1.21×10^{-2}	-3.34×10^{-3}	7.6×10^{-6}	7.6×10^{-6}
6	-1.39×10^{-2}	-1.68×10^{-2}	8.4×10^{-7}	1.5×10^{-6}
8	-1.46×10^{-2}	-3.01×10^{-2}	1.6×10^{-7}	4.1×10^{-7}
10	-1.53×10^{-2}	-3.97×10^{-2}	4.4×10^{-8}	1.4×10^{-7}

Note that part of the off-shell corrections in the model of Ref. [14] are included in the relativistic distribution function (11), which in the model of Ref. [25] are contained only in the non-convolution term. Therefore the definition of off-shell corrections can differ between various models, and one should ensure that off-shell effects in general are calculated self-consistently. The difference between the two models provides an estimate of the systematic error associated with the poor knowledge of the change in the nucleon structure when the nucleon is bound in deuteron.

2.4 Small- x effects: shadowing and meson exchange currents

For completeness, in this section we briefly discuss the nuclear corrections in the deuteron at small values of x . From the definition of the moments of the F_2 structure function, it is clear that small- x effects will mostly be relevant for the lowest moment, and will be negligible for $n \geq 4$.

At small values of x , the coherence length of a virtual $q\bar{q}$ fluctuation of the photon probe in the laboratory frame is $\sim 1/Mx$, which for $x \lesssim 0.1$ becomes larger than the inter-nucleon separation. Consequently at small x the scattering from the deuteron can take place via double scattering from both nucleons, which gives rise to the phenomenon of nuclear shadowing (see e.g. Refs. [4, 2]).

At low Q^2 the $q\bar{q}$ fluctuations are usually represented in the form of the vector mesons, ρ , ω and ϕ . Their contributions scale as $1/Q^2$, however, and are formally of higher twist. Leading twist shadowing contributions arise from diffractive scattering of the virtual photon from the bound nucleons, which is described through Pomeron exchange, as well as contributions in which the exchanged quanta are mesons (most notably the pion).

Both the Pomeron (P) exchange and meson exchange current (MEC) contributions to the deuteron F_2^D structure function have been estimated by several authors [1, 2, 3, 4, 25, 26], and enter as additive corrections to F_2^D ,

$$F_2^D(x, Q^2) \rightarrow F_2^D(x, Q^2) + \delta^{(P, \text{MEC})} F_2^D(x, Q^2). \quad (30)$$

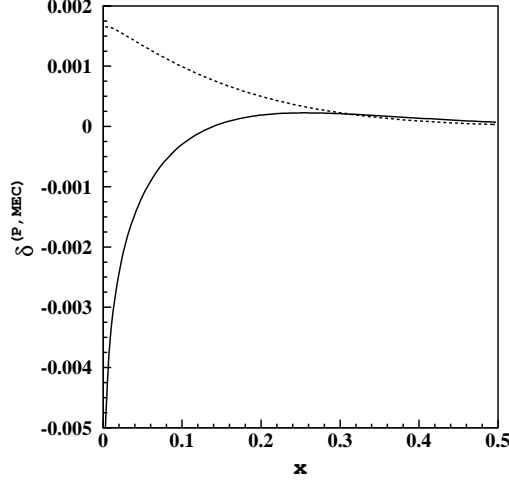


Figure 5: Shadowing (Pomeron exchange) and meson exchange current corrections $\delta^{(P)}(x, Q^2)$ (solid) and $\delta^{(\text{MEC})}(x, Q^2)$ (dotted) as a function of x at $Q^2 = 10 \text{ GeV}^2$ [3].

The Pomeron shadowing contribution $\delta^{(P)} F_2^D$ is negative, while the meson (pion) exchange contribution $\delta^{(\text{MEC})} F_2^D$ is positive and hence corresponds to an antishadowing effect. To estimate their effect on the moment analysis, we use the results from Ref. [3], which can be conveniently parameterized at $Q^2 \sim 5 \text{ GeV}^2$ as

$$\delta^{(P)} F_2^D = b_0 x^{b_1} (1-x)^{b_2} (1 + b_3 x^{b_4}) , \quad (31)$$

for the P -exchange, where $b_0 = -0.003$, $b_1 = -0.13$, $b_2 = 5.0$, $b_3 = -2.2$ and $b_4 = 0.4$, and

$$\delta^{(\text{MEC})} F_2^D = c_0 x^{c_1} (1-x)^{c_2} \quad (32)$$

for meson exchange, with $c_0 = 0.002$, $c_1 = 0.03$ and $c_2 = 6.0$. As a fraction of the empirical leading twist F_2^D , the ratios

$$\delta^{(P, \text{MEC})}(x, Q^2) = \frac{\delta^{(P, \text{MEC})} F_2^D(x, Q^2)}{F_2^D(x, Q^2)} \quad (33)$$

are plotted in Fig. 5. The corresponding moments, defined in analogy with Eq. (26),

$$\Delta_n^{(P, \text{MEC})}(Q^2) = \frac{1}{M_n^D} \int dx x^{n-2} \delta^{(P, \text{MEC})}(x, Q^2) F_2^D(x, Q^2) , \quad (34)$$

are listed in Table 1, where it is clear that these corrections are negligible for $n \geq 4$.

3 Moments of the neutron structure function

In this section we present the extraction of the lowest few moments of the neutron structure function F_2^n , taking into account the systematic uncertainties associated with our incomplete knowledge of nuclear effects in the deuteron. We shall focus on the leading twist (LT) part of the structure function, and make use of the previous determination of the LT moments of the proton and deuteron structure functions obtained by the twist analyses of Refs. [5, 6]. Higher twist contributions to the moments, in the form of subleading $1/Q^2$ power corrections, will be discussed in Sec. 4. Moreover, since the twist extraction performed in Refs. [5, 6] is based on the Nachtmann definition of the moments [23], our LT terms are determined without any *a priori* knowledge of the x -shape of parton distribution functions (PDFs).

The moments of the LT F_2 structure function of the neutron are related to those of proton and deuteron by

$$M_n^n(Q^2) = 2M_n^D(Q^2) \frac{1 - \Delta_n^{(\text{off})}(Q^2) - \Delta_n^{(P,\text{MEC})}(Q^2)}{\mathcal{F}_n^D} - M_n^P(Q^2), \quad (35)$$

where $\mathcal{F}_n^D/[1 - \Delta_n^{(\text{off})}(Q^2) - \Delta_n^{(P,\text{MEC})}(Q^2)]$ represents the nuclear correction factor, or in other words the EMC effect of the deuteron in moment space. From the values reported in Fig. 2 and in Table 1, the EMC effect on the second moment is expected to be below 1% [see also Fig. 3(a)].

Using the nuclear ingredients discussed in the previous Section, the extracted LT moments $M_n^n(Q^2)$ are listed in Table 2 and shown in Fig. 6. The central values refer to the case of the relativistic distribution (11) with the deuteron wave function from Ref. [12]. For comparison we also plot the corresponding proton (stars) and deuteron (open crosses) LT moments. It turns out that the neutron LT moments with $n \leq 8$ can be determined with quite good precision, namely $\leq 18\%$ (statistical) and $\leq 30\%$ (systematic). Different contributions to the total systematic error are shown in Fig. 7. It can be seen that all the uncertainties related to the nuclear correction factor steeply rise with n , so that the total errors due to nuclear effects become comparable with the experimental ones around $n = 10$. Thus, an improvement in the measurements of the proton and deuteron structure functions at large x would be beneficial and also the moments at $n = 12$ may be still reasonably accessible.

In Fig. 8 our extracted neutron moments are compared with the corresponding moments calculated from various PDF sets available in the literature [27, 28, 29, 30]. For $n > 2$ all PDF sets predict significantly lower moments at low Q^2 . This difference is due to Sudakov effects at large- x ; indeed, as was firstly investigated in Ref. [31], soft gluon resummation plays a relevant role for $n > 2$ already at $Q^2 = 3 - 4 \text{ GeV}^2$. While resummation effects are taken into account in the analysis of Refs. [5, 6], all the PDF sets of Refs. [27, 28, 29, 30] are based on next-to-leading (NLO) or NNLO treatments. At higher Q^2 the PDF predictions are consistent with our results for $n \leq 10$ within the quoted statistical errors. For M_2 however all PDFs give somehow smaller values at large Q^2 , though within the statistical uncertainties.

Table 2: *Extracted leading twist moments of the neutron F_2 structure functions, $M_n^n(Q^2)$, for $n = 2, 4, 6, 8$, shown in Fig. 6, together with statistical and systematic uncertainties.*

Q^2 [(GeV/c) 2]	$M_2^n(Q^2) \times 10^{-1}$	$M_4^n(Q^2) \times 10^{-2}$	$M_6^n(Q^2) \times 10^{-3}$	$M_8^n(Q^2) \times 10^{-3}$
1.025	1.37 ± 0.06 ± 0.12	1.95 ± 0.20 ± 0.11	8.06 ± 0.45 ± 1.15	5.51 ± 0.98 ± 1.49
1.075	1.36 ± 0.06 ± 0.12	1.88 ± 0.19 ± 0.11	7.35 ± 0.41 ± 1.04	4.59 ± 0.81 ± 1.24
1.125	1.36 ± 0.06 ± 0.12	1.82 ± 0.18 ± 0.11	6.78 ± 0.38 ± 0.96	3.95 ± 0.70 ± 1.07
1.175	1.36 ± 0.06 ± 0.12	1.76 ± 0.18 ± 0.10	6.33 ± 0.35 ± 0.90	3.48 ± 0.62 ± 0.94
1.225	1.36 ± 0.05 ± 0.11	1.71 ± 0.17 ± 0.10	5.95 ± 0.33 ± 0.85	3.13 ± 0.56 ± 0.85
1.275	1.35 ± 0.05 ± 0.11	1.67 ± 0.17 ± 0.10	5.63 ± 0.31 ± 0.80	2.85 ± 0.51 ± 0.77
1.325	1.35 ± 0.05 ± 0.11	1.63 ± 0.16 ± 0.09	5.36 ± 0.30 ± 0.76	2.63 ± 0.47 ± 0.71
1.375	1.35 ± 0.05 ± 0.11	1.59 ± 0.16 ± 0.09	5.13 ± 0.28 ± 0.73	2.44 ± 0.43 ± 0.66
1.425	1.34 ± 0.05 ± 0.11	1.56 ± 0.16 ± 0.09	4.93 ± 0.27 ± 0.70	2.29 ± 0.41 ± 0.62
1.475	1.34 ± 0.05 ± 0.11	1.53 ± 0.15 ± 0.09	4.74 ± 0.26 ± 0.68	2.16 ± 0.38 ± 0.58
1.525	1.34 ± 0.05 ± 0.11	1.50 ± 0.15 ± 0.09	4.58 ± 0.25 ± 0.65	2.04 ± 0.36 ± 0.55
1.575	1.34 ± 0.05 ± 0.11	1.48 ± 0.15 ± 0.09	4.44 ± 0.25 ± 0.63	1.94 ± 0.35 ± 0.53
1.625	1.33 ± 0.05 ± 0.11	1.45 ± 0.15 ± 0.08	4.31 ± 0.24 ± 0.61	1.86 ± 0.33 ± 0.50
1.675	1.33 ± 0.05 ± 0.11	1.43 ± 0.14 ± 0.08	4.19 ± 0.23 ± 0.60	1.78 ± 0.32 ± 0.48
1.725	1.33 ± 0.05 ± 0.11	1.41 ± 0.14 ± 0.08	4.08 ± 0.23 ± 0.58	1.71 ± 0.30 ± 0.46
1.775	1.32 ± 0.05 ± 0.11	1.39 ± 0.14 ± 0.08	3.99 ± 0.22 ± 0.57	1.65 ± 0.29 ± 0.45
1.825	1.32 ± 0.05 ± 0.11	1.37 ± 0.14 ± 0.08	3.90 ± 0.22 ± 0.55	1.60 ± 0.28 ± 0.43
1.875	1.32 ± 0.05 ± 0.11	1.36 ± 0.14 ± 0.08	3.81 ± 0.21 ± 0.54	1.55 ± 0.27 ± 0.42
1.925	1.32 ± 0.05 ± 0.11	1.34 ± 0.13 ± 0.08	3.73 ± 0.21 ± 0.53	1.50 ± 0.27 ± 0.41
1.975	1.32 ± 0.05 ± 0.11	1.33 ± 0.13 ± 0.08	3.66 ± 0.20 ± 0.52	1.46 ± 0.26 ± 0.40
2.025	1.31 ± 0.05 ± 0.11	1.31 ± 0.13 ± 0.08	3.59 ± 0.20 ± 0.51	1.42 ± 0.25 ± 0.38
2.075	1.31 ± 0.05 ± 0.11	1.30 ± 0.13 ± 0.08	3.53 ± 0.20 ± 0.50	1.38 ± 0.25 ± 0.38
2.125	1.31 ± 0.05 ± 0.11	1.29 ± 0.13 ± 0.07	3.47 ± 0.19 ± 0.49	1.35 ± 0.24 ± 0.37
2.175	1.31 ± 0.05 ± 0.10	1.27 ± 0.13 ± 0.07	3.42 ± 0.19 ± 0.49	1.32 ± 0.23 ± 0.36
2.225	1.31 ± 0.05 ± 0.10	1.26 ± 0.13 ± 0.07	3.36 ± 0.19 ± 0.48	1.29 ± 0.23 ± 0.35
2.275	1.31 ± 0.05 ± 0.10	1.25 ± 0.13 ± 0.07	3.32 ± 0.18 ± 0.47	1.27 ± 0.22 ± 0.34
2.325	1.31 ± 0.05 ± 0.10	1.24 ± 0.12 ± 0.07	3.28 ± 0.18 ± 0.47	1.25 ± 0.22 ± 0.34
2.375	1.30 ± 0.05 ± 0.10	1.23 ± 0.12 ± 0.07	3.24 ± 0.18 ± 0.46	1.23 ± 0.22 ± 0.33
2.425	1.30 ± 0.05 ± 0.10	1.22 ± 0.12 ± 0.07	3.20 ± 0.18 ± 0.46	1.21 ± 0.21 ± 0.33
2.475	1.30 ± 0.05 ± 0.10	1.22 ± 0.12 ± 0.07	3.17 ± 0.18 ± 0.45	1.19 ± 0.21 ± 0.32
2.525	1.30 ± 0.05 ± 0.10	1.21 ± 0.12 ± 0.07	3.13 ± 0.17 ± 0.45	1.17 ± 0.21 ± 0.32
2.575	1.30 ± 0.05 ± 0.10	1.20 ± 0.12 ± 0.07	3.10 ± 0.17 ± 0.44	1.15 ± 0.21 ± 0.31
2.625	1.30 ± 0.05 ± 0.10	1.19 ± 0.12 ± 0.07	3.07 ± 0.17 ± 0.44	1.14 ± 0.20 ± 0.31
2.675	1.30 ± 0.05 ± 0.10	1.18 ± 0.12 ± 0.07	3.04 ± 0.17 ± 0.43	1.12 ± 0.20 ± 0.30
2.725	1.30 ± 0.05 ± 0.10	1.18 ± 0.12 ± 0.07	3.01 ± 0.17 ± 0.43	1.11 ± 0.20 ± 0.30
2.775	1.30 ± 0.05 ± 0.10	1.17 ± 0.12 ± 0.07	2.98 ± 0.17 ± 0.42	1.10 ± 0.19 ± 0.30
2.825	1.30 ± 0.05 ± 0.10	1.16 ± 0.12 ± 0.07	2.96 ± 0.16 ± 0.42	1.08 ± 0.19 ± 0.29
2.875	1.30 ± 0.05 ± 0.10	1.16 ± 0.12 ± 0.07	2.93 ± 0.16 ± 0.42	1.07 ± 0.19 ± 0.29
2.925	1.30 ± 0.05 ± 0.10	1.15 ± 0.12 ± 0.07	2.91 ± 0.16 ± 0.41	1.06 ± 0.19 ± 0.29
2.975	1.30 ± 0.05 ± 0.10	1.15 ± 0.12 ± 0.07	2.88 ± 0.16 ± 0.41	1.05 ± 0.19 ± 0.28
3.025	1.30 ± 0.05 ± 0.10	1.14 ± 0.11 ± 0.07	2.86 ± 0.16 ± 0.41	1.04 ± 0.18 ± 0.28
3.075	1.30 ± 0.05 ± 0.10	1.13 ± 0.11 ± 0.07	2.84 ± 0.16 ± 0.40	1.03 ± 0.18 ± 0.28
3.125	1.30 ± 0.05 ± 0.10	1.13 ± 0.11 ± 0.07	2.82 ± 0.16 ± 0.40	1.02 ± 0.18 ± 0.28
3.175	1.30 ± 0.05 ± 0.10	1.12 ± 0.11 ± 0.07	2.80 ± 0.16 ± 0.40	1.01 ± 0.18 ± 0.27
3.225	1.30 ± 0.05 ± 0.10	1.12 ± 0.11 ± 0.06	2.78 ± 0.15 ± 0.40	1.00 ± 0.18 ± 0.27
3.275	1.30 ± 0.05 ± 0.10	1.11 ± 0.11 ± 0.06	2.76 ± 0.15 ± 0.39	0.99 ± 0.18 ± 0.27
3.325	1.30 ± 0.05 ± 0.10	1.11 ± 0.11 ± 0.06	2.74 ± 0.15 ± 0.39	0.98 ± 0.17 ± 0.27
3.375	1.30 ± 0.05 ± 0.10	1.10 ± 0.11 ± 0.06	2.72 ± 0.15 ± 0.39	0.97 ± 0.17 ± 0.26
3.425	1.30 ± 0.05 ± 0.10	1.10 ± 0.11 ± 0.06	2.70 ± 0.15 ± 0.38	0.96 ± 0.17 ± 0.26
3.475	1.30 ± 0.05 ± 0.10	1.09 ± 0.11 ± 0.06	2.68 ± 0.15 ± 0.38	0.95 ± 0.17 ± 0.26
3.525	1.29 ± 0.05 ± 0.10	1.09 ± 0.11 ± 0.06	2.67 ± 0.15 ± 0.38	0.94 ± 0.17 ± 0.26
3.575	1.29 ± 0.05 ± 0.10	1.08 ± 0.11 ± 0.06	2.65 ± 0.15 ± 0.38	0.94 ± 0.17 ± 0.25
3.625	1.29 ± 0.05 ± 0.10	1.08 ± 0.11 ± 0.06	2.64 ± 0.15 ± 0.38	0.93 ± 0.17 ± 0.25
3.675	1.29 ± 0.05 ± 0.10	1.08 ± 0.11 ± 0.06	2.62 ± 0.15 ± 0.37	0.92 ± 0.16 ± 0.25
3.725	1.29 ± 0.05 ± 0.10	1.07 ± 0.11 ± 0.06	2.60 ± 0.14 ± 0.37	0.92 ± 0.16 ± 0.25
3.775	1.29 ± 0.05 ± 0.10	1.07 ± 0.11 ± 0.06	2.59 ± 0.14 ± 0.37	0.91 ± 0.16 ± 0.25
3.825	1.29 ± 0.05 ± 0.10	1.06 ± 0.11 ± 0.06	2.58 ± 0.14 ± 0.37	0.90 ± 0.16 ± 0.24

Q^2 [(GeV/c) ²]	$M_2^n(Q^2) \times 10^{-1}$	$M_4^n(Q^2) \times 10^{-2}$	$M_6^n(Q^2) \times 10^{-3}$	$M_8^n(Q^2) \times 10^{-3}$
3.875	1.29 ± 0.05 ± 0.10	1.06 ± 0.11 ± 0.06	2.56 ± 0.14 ± 0.36	0.90 ± 0.16 ± 0.24
3.925	1.29 ± 0.05 ± 0.10	1.06 ± 0.11 ± 0.06	2.55 ± 0.14 ± 0.36	0.89 ± 0.16 ± 0.24
3.975	1.29 ± 0.05 ± 0.10	1.05 ± 0.11 ± 0.06	2.53 ± 0.14 ± 0.36	0.88 ± 0.16 ± 0.24
4.025	1.29 ± 0.05 ± 0.10	1.05 ± 0.11 ± 0.06	2.52 ± 0.14 ± 0.36	0.88 ± 0.16 ± 0.24
4.075	1.29 ± 0.05 ± 0.10	1.05 ± 0.11 ± 0.06	2.51 ± 0.14 ± 0.36	0.87 ± 0.15 ± 0.24
4.125	1.29 ± 0.05 ± 0.10	1.04 ± 0.10 ± 0.06	2.50 ± 0.14 ± 0.36	0.87 ± 0.15 ± 0.23
4.175	1.29 ± 0.05 ± 0.10	1.04 ± 0.10 ± 0.06	2.48 ± 0.14 ± 0.35	0.86 ± 0.15 ± 0.23
4.225	1.29 ± 0.05 ± 0.10	1.04 ± 0.10 ± 0.06	2.47 ± 0.14 ± 0.35	0.86 ± 0.15 ± 0.23
4.275	1.29 ± 0.05 ± 0.10	1.03 ± 0.10 ± 0.06	2.46 ± 0.14 ± 0.35	0.85 ± 0.15 ± 0.23
4.325	1.29 ± 0.05 ± 0.10	1.03 ± 0.10 ± 0.06	2.45 ± 0.14 ± 0.35	0.84 ± 0.15 ± 0.23
4.375	1.29 ± 0.05 ± 0.10	1.03 ± 0.10 ± 0.06	2.44 ± 0.14 ± 0.35	0.84 ± 0.15 ± 0.23
4.425	1.29 ± 0.05 ± 0.10	1.02 ± 0.10 ± 0.06	2.43 ± 0.13 ± 0.35	0.84 ± 0.15 ± 0.23
4.475	1.29 ± 0.05 ± 0.10	1.02 ± 0.10 ± 0.06	2.42 ± 0.13 ± 0.34	0.83 ± 0.15 ± 0.23
4.525	1.29 ± 0.05 ± 0.10	1.02 ± 0.10 ± 0.06	2.41 ± 0.13 ± 0.34	0.83 ± 0.15 ± 0.22
4.575	1.29 ± 0.05 ± 0.10	1.01 ± 0.10 ± 0.06	2.40 ± 0.13 ± 0.34	0.82 ± 0.15 ± 0.22
4.625	1.29 ± 0.05 ± 0.10	1.01 ± 0.10 ± 0.06	2.39 ± 0.13 ± 0.34	0.82 ± 0.15 ± 0.22
4.675	1.29 ± 0.05 ± 0.10	1.01 ± 0.10 ± 0.06	2.38 ± 0.13 ± 0.34	0.81 ± 0.14 ± 0.22
4.725	1.29 ± 0.05 ± 0.10	1.01 ± 0.10 ± 0.06	2.37 ± 0.13 ± 0.34	0.81 ± 0.14 ± 0.22
4.775	1.29 ± 0.05 ± 0.10	1.00 ± 0.10 ± 0.06	2.36 ± 0.13 ± 0.34	0.80 ± 0.14 ± 0.22
4.825	1.29 ± 0.05 ± 0.10	1.00 ± 0.10 ± 0.06	2.35 ± 0.13 ± 0.33	0.80 ± 0.14 ± 0.22
4.875	1.29 ± 0.05 ± 0.10	1.00 ± 0.10 ± 0.06	2.34 ± 0.13 ± 0.33	0.80 ± 0.14 ± 0.22
4.925	1.29 ± 0.05 ± 0.10	1.00 ± 0.10 ± 0.06	2.33 ± 0.13 ± 0.33	0.79 ± 0.14 ± 0.21
4.975	1.29 ± 0.05 ± 0.10	0.99 ± 0.10 ± 0.06	2.32 ± 0.13 ± 0.33	0.79 ± 0.14 ± 0.21
5.025	1.29 ± 0.05 ± 0.10	0.99 ± 0.10 ± 0.06	2.31 ± 0.13 ± 0.33	0.78 ± 0.14 ± 0.21
5.075	1.29 ± 0.05 ± 0.10	0.99 ± 0.10 ± 0.06	2.30 ± 0.13 ± 0.33	0.78 ± 0.14 ± 0.21
5.125	1.29 ± 0.05 ± 0.10	0.99 ± 0.10 ± 0.06	2.30 ± 0.13 ± 0.33	0.78 ± 0.14 ± 0.21
5.275	1.29 ± 0.05 ± 0.10	0.98 ± 0.10 ± 0.06	2.27 ± 0.13 ± 0.32	0.77 ± 0.14 ± 0.21
5.325	1.29 ± 0.05 ± 0.10	0.98 ± 0.10 ± 0.06	2.26 ± 0.13 ± 0.32	0.76 ± 0.14 ± 0.21
5.375	1.29 ± 0.05 ± 0.10	0.97 ± 0.10 ± 0.06	2.26 ± 0.13 ± 0.32	0.76 ± 0.13 ± 0.21
5.475	1.28 ± 0.05 ± 0.09	0.97 ± 0.10 ± 0.06	2.24 ± 0.12 ± 0.32	0.75 ± 0.13 ± 0.20
5.525	1.28 ± 0.05 ± 0.09	0.97 ± 0.10 ± 0.06	2.23 ± 0.12 ± 0.32	0.75 ± 0.13 ± 0.20
5.625	1.28 ± 0.05 ± 0.09	0.96 ± 0.10 ± 0.06	2.22 ± 0.12 ± 0.32	0.74 ± 0.13 ± 0.20
5.675	1.28 ± 0.05 ± 0.09	0.96 ± 0.10 ± 0.06	2.21 ± 0.12 ± 0.31	0.74 ± 0.13 ± 0.20
5.725	1.28 ± 0.05 ± 0.09	0.96 ± 0.10 ± 0.06	2.21 ± 0.12 ± 0.31	0.74 ± 0.13 ± 0.20
5.955	1.28 ± 0.05 ± 0.09	0.95 ± 0.10 ± 0.06	2.18 ± 0.12 ± 0.31	0.72 ± 0.13 ± 0.20
6.915	1.28 ± 0.04 ± 0.09	0.92 ± 0.09 ± 0.05	2.07 ± 0.12 ± 0.29	0.68 ± 0.12 ± 0.18
7.267	1.28 ± 0.04 ± 0.09	0.91 ± 0.09 ± 0.05	2.04 ± 0.11 ± 0.29	0.67 ± 0.12 ± 0.18
7.630	1.28 ± 0.04 ± 0.09	0.90 ± 0.09 ± 0.05	2.00 ± 0.11 ± 0.29	0.65 ± 0.12 ± 0.18
8.021	1.28 ± 0.04 ± 0.09	0.89 ± 0.09 ± 0.05	1.97 ± 0.11 ± 0.28	0.64 ± 0.11 ± 0.17
8.847	1.28 ± 0.04 ± 0.09	0.87 ± 0.09 ± 0.05	1.91 ± 0.11 ± 0.27	0.62 ± 0.11 ± 0.17
9.775	1.27 ± 0.04 ± 0.09	0.85 ± 0.09 ± 0.05	1.86 ± 0.10 ± 0.26	0.59 ± 0.11 ± 0.16
10.267	1.27 ± 0.04 ± 0.09	0.85 ± 0.09 ± 0.05	1.83 ± 0.10 ± 0.26	0.58 ± 0.10 ± 0.16
10.762	1.27 ± 0.04 ± 0.09	0.84 ± 0.08 ± 0.05	1.81 ± 0.10 ± 0.26	0.57 ± 0.10 ± 0.16
11.344	1.27 ± 0.04 ± 0.09	0.83 ± 0.08 ± 0.05	1.78 ± 0.10 ± 0.25	0.56 ± 0.10 ± 0.15
12.580	1.27 ± 0.04 ± 0.09	0.81 ± 0.08 ± 0.05	1.73 ± 0.10 ± 0.25	0.54 ± 0.10 ± 0.15
13.238	1.27 ± 0.04 ± 0.09	0.80 ± 0.08 ± 0.05	1.71 ± 0.10 ± 0.24	0.53 ± 0.09 ± 0.15
14.689	1.27 ± 0.04 ± 0.09	0.79 ± 0.08 ± 0.05	1.66 ± 0.09 ± 0.24	0.52 ± 0.09 ± 0.14
17.108	1.26 ± 0.04 ± 0.09	0.77 ± 0.08 ± 0.04	1.60 ± 0.09 ± 0.23	0.49 ± 0.09 ± 0.13
19.072	1.26 ± 0.04 ± 0.09	0.75 ± 0.08 ± 0.04	1.56 ± 0.09 ± 0.22	0.48 ± 0.08 ± 0.13
20.108	1.26 ± 0.04 ± 0.09	0.75 ± 0.08 ± 0.04	1.54 ± 0.09 ± 0.22	0.47 ± 0.08 ± 0.13
21.097	1.26 ± 0.04 ± 0.09	0.74 ± 0.07 ± 0.04	1.52 ± 0.08 ± 0.22	0.46 ± 0.08 ± 0.13
24.259	1.26 ± 0.04 ± 0.08	0.73 ± 0.07 ± 0.04	1.47 ± 0.08 ± 0.21	0.44 ± 0.08 ± 0.12
26.680	1.26 ± 0.04 ± 0.08	0.71 ± 0.07 ± 0.04	1.44 ± 0.08 ± 0.21	0.43 ± 0.08 ± 0.12
32.500	1.25 ± 0.04 ± 0.08	0.69 ± 0.07 ± 0.04	1.39 ± 0.08 ± 0.20	0.41 ± 0.07 ± 0.11
34.932	1.25 ± 0.04 ± 0.08	0.69 ± 0.07 ± 0.04	1.37 ± 0.08 ± 0.19	0.41 ± 0.07 ± 0.11
36.750	1.25 ± 0.04 ± 0.08	0.68 ± 0.07 ± 0.04	1.35 ± 0.08 ± 0.19	0.40 ± 0.07 ± 0.11
43.970	1.25 ± 0.04 ± 0.08	0.66 ± 0.07 ± 0.04	1.31 ± 0.07 ± 0.19	0.38 ± 0.07 ± 0.10
47.440	1.25 ± 0.04 ± 0.08	0.66 ± 0.07 ± 0.04	1.29 ± 0.07 ± 0.18	0.38 ± 0.07 ± 0.10
64.270	1.25 ± 0.04 ± 0.08	0.63 ± 0.06 ± 0.04	1.22 ± 0.07 ± 0.17	0.35 ± 0.06 ± 0.10
75.000	1.25 ± 0.04 ± 0.08	0.62 ± 0.06 ± 0.04	1.19 ± 0.07 ± 0.17	0.34 ± 0.06 ± 0.09
86.000	1.24 ± 0.04 ± 0.08	0.61 ± 0.06 ± 0.04	1.16 ± 0.06 ± 0.17	0.33 ± 0.06 ± 0.09
97.690	1.24 ± 0.04 ± 0.08	0.60 ± 0.06 ± 0.03	1.13 ± 0.06 ± 0.16	0.32 ± 0.06 ± 0.09

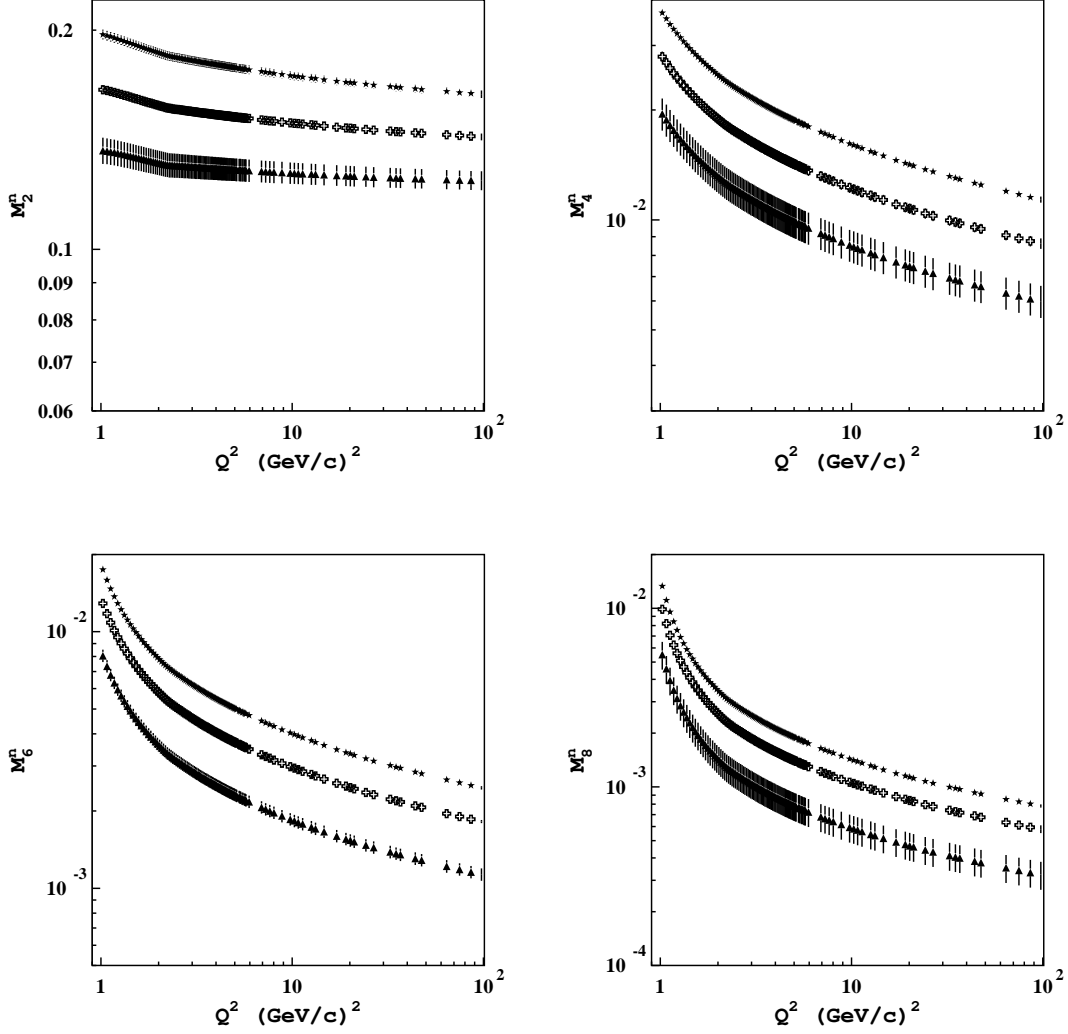


Figure 6: *Leading twist moments of the neutron structure function for $n = 2, 4, 6$ and 8 as a function of Q^2 (triangles), extracted using the relativistic distribution in Eq. (11) with the deuteron wave function from Ref. [12]. For comparison we also show the proton (stars) and deuteron (open crosses) moments. The errors shown are statistical.*

The large- n behavior of the moments is also closely related to the asymptotic $x \rightarrow 1$ behavior of the structure functions. Indeed, inspecting the definition of the moments, Eq. (2), we conclude that at $n \gg 1$ the factor x^{n-2} in the integrand suppresses the contribution from the region of small x , leaving the moment effectively saturated by a region close to $x = 1$. Furthermore, assuming that the structure functions F_2^p and F_2^n vanish as $(1-x)^\beta$ with the same exponent for the proton and neutron (as one would

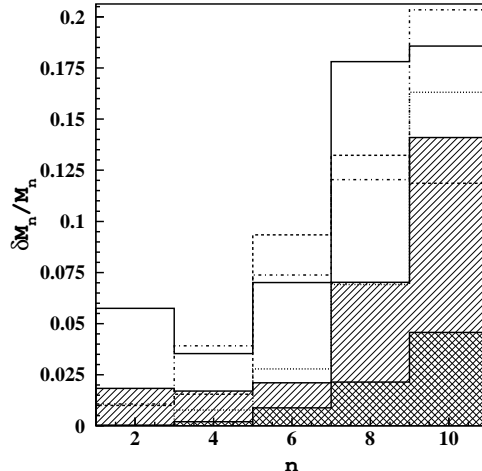


Figure 7: Various contributions to the systematic errors on the LT neutron moments for $n = 2 - 10$: deuteron LT moment error (solid); proton LT moment error (dashed); error due to the momentum cut (dotted); dependence on the relativistic treatment (dot-dashed); offshellness uncertainty (left-hatched); wave function model dependence (cross-hatched).

expect from perturbative QCD) [32], it is possible to derive the asymptotic relation between the ratios of the moments and the structure functions

$$\lim_{n \rightarrow \infty} \frac{M_n^n}{M_n^p} = \lim_{x \rightarrow 1} \frac{F_2^n(x)}{F_2^p(x)}. \quad (36)$$

This relation can be useful in obtaining some insights into the large- x asymptotics of the d/u ratio from the large- n limit of the neutron and proton moments. Note that most of the PDF fits [27, 28, 29, 30] are characterized by the limiting value $\lim_{x \rightarrow 1} F_2^n/F_2^p = 1/4$, which is expected if soft, nonperturbative effects dominate the scattering at large x (namely, if the energy of the spectator uu system which accompanies the d quark is increased relative to the ud system which is relevant for the u quark [33]). On the other hand, arguments based on helicity conservation in pQCD, when combined with an unperturbed spin-flavor symmetric wave function, suggest an asymptotic value of $3/7$ [34].

The ratios of neutron to proton LT moments are shown in Fig. 9 for several n , where they are also compared to various PDF parameterizations [27, 28, 29, 30]. The ratio depends only slightly on Q^2 for $n = 2$, while it is almost completely Q^2 -independent for larger n . The latter are in reasonable agreement with our extracted ratios within both statistical and systematical errors.

The n/p ratio systematically decreases with n and reaches the value $\simeq 0.34 \pm 0.12_{\text{stat}} \pm 0.13_{\text{syst}}$ at $n = 10$. To compare this with the theoretical predictions the mean value of x

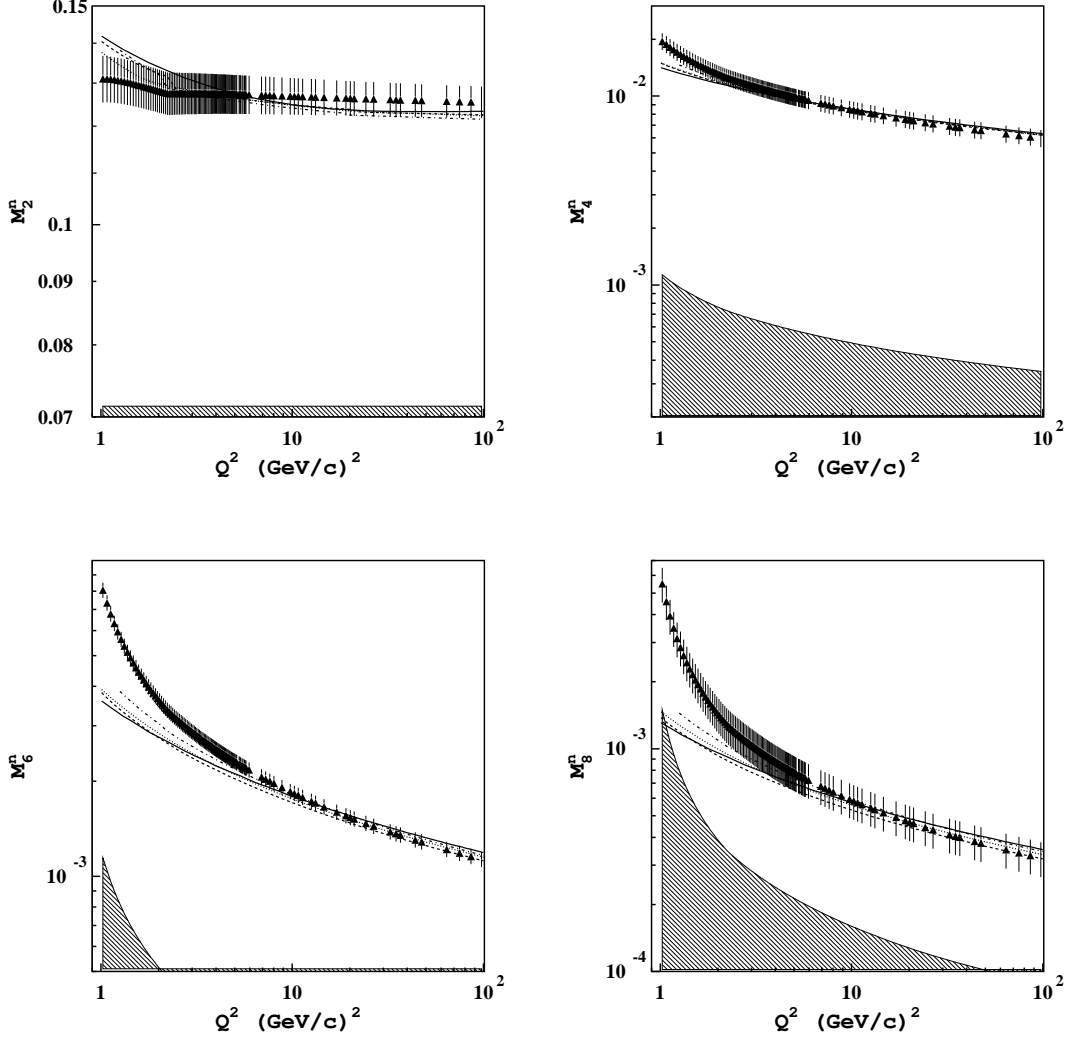


Figure 8: *Extracted moments of the neutron structure function for $n = 2, 4, 6$ and 8 as a function of Q^2 in comparison to moments of different PDFs: solid line represents GRV [27], dashed line represents Alekhin [30], dotted line represents CTEQ [29], dot-dashed line represents MRST [28]. The hatched area shows systematic errors.*

probed by our moments needs to be estimated. This can be done in the following way: for any calculated n -th neutron and proton moment we estimate a corresponding average value of x defined as $\langle x \rangle_n \equiv (M_{n+1}^n + M_{n+1}^p)/(M_n^n + M_n^p)$; then the ratio of neutron to proton structure functions is computed at the values $\langle x \rangle_n$.

The results of this procedure are shown in Fig. 10 (dashed curve), where they are also compared with the ratio of the extracted LT moments (solid curve). The two ratios

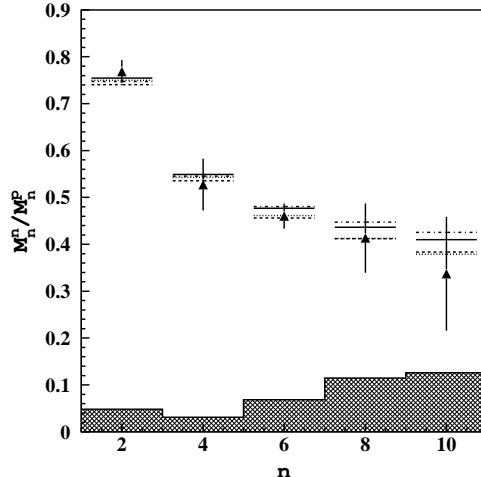


Figure 9: Ratio of neutron to proton leading twist moments for various n (triangles), together with the statistical and systematic uncertainties (hatched area). The horizontal lines denote the ratios obtained with different PDF sets: GRV [27] (solid), Alekhin [30] (dashed), CTEQ [29] (dotted), MRST [28] (dot-dashed).

coincide with good accuracy, suggesting that the extracted ratio of moments is similar to the ratio of structure functions taken at the average value $\langle x \rangle_n$. Note that at $n = 10$ one has $\langle x \rangle_{10} \simeq 0.70$, and the F_2^n/F_2^p ratio at $x \simeq 0.70$ is equal to $0.34 \pm 0.12_{\text{stat}} \pm 0.13_{\text{sys}}$. As discussed above (see Fig. 7), moments for $n = 12$ may still be accessible by improving measurements of the proton and deuteron structure functions at large x , and with $n = 12$ one can probe values of x as large as 0.75. However, higher $\langle x \rangle_n$ values are difficult to access by this method because of the rapid increase of the uncertainties on the nuclear corrections with the order n .

The sensitivity of the moment's ratio to the high- x tail of the PDFs is illustrated in Fig. 11, where our n/p moment's ratio (triangles) is compared with the PDF parameterizations from Ref. [29] with and without modifying the d -quark distribution as:

$$d(x) \rightarrow d(x) + 0.1 x^m (1+x) u(x). \quad (37)$$

with m a parameter. Depending on the value of m , the form in Eq. (37) allows the $x \rightarrow 1$ behavior of the d/u ratio to vary between 0 and $1/5$, which correspond respectively to the structure function limits $\lim_{x \rightarrow 1} F_2^n(x)/F_2^p(x)$ of $1/4$ and $3/7$. The dotted line in Fig. 11 corresponds to the case $m = 1$ in Eq. (37), which was advocated in the NNLO analysis of both electron and neutrino DIS data of Ref. [35]. It appears that our results rule out such an enhancement of the d quark distribution, since the correction is not negligible even at values of x as low as $x \simeq 0.5$. A larger value of the parameter m confines the enhancement only to larger values of x , and the results obtained adopting

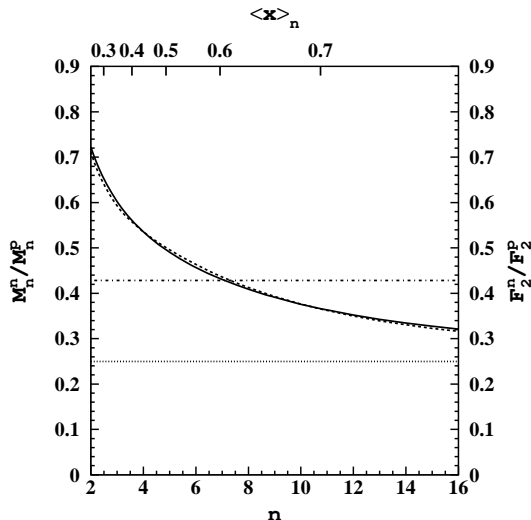


Figure 10: Ratio of extracted neutron to proton leading twist moments as a function of n (solid), compared with the structure function ratio (dashed) evaluated using the PDFs of Ref. [29], as a function of $\langle x \rangle_n$ (top axis). The horizontal lines denote the asymptotic $x \rightarrow 1$ values for the structure function moments of $1/4$ [33] and $3/7$ [34].

value $m = 4$, corresponding to the dashed line in Fig. 11, are more consistent with our extracted n/p ratio.

Before closing this section, our results for the LT moments of the nonsinglet $p - n$ part of the F_2 structure function, $M_n^{p-n}(Q^2) = M_n^p(Q^2) - M_n^n(Q^2)$, are listed in Table 3 together with their statistical and systematic uncertainties. We point out that an important fraction of the total systematic error for the second moments $M_2^p(Q^2)$ and $M_2^n(Q^2)$ comes from the extrapolation in the unmeasured low- x regions. Such systematic uncertainty basically cancels out in the isovector $p - n$ combination. This allows us to determine $M_2^{p-n}(Q^2)$ within $\approx 20\%$ global accuracy.

Low-order moments of the isovector $u - d$ quark distributions have been recently calculated in both unquenched [36] and quenched [37] lattice QCD. Our results for the nonsinglet LT moments M_n^{p-n} can be easily compared with those of the isovector moments ($\langle x^{n-1} \rangle_u - \langle x^{n-1} \rangle_d$), taking into account that for even values of the order n one has

$$M_n^{p-n}(Q^2) = \frac{1}{3} C_n^{NS} (\langle x^{n-1} \rangle_u - \langle x^{n-1} \rangle_d) , \quad (38)$$

where C_n^{NS} is the $(n - 1)$ -th moment of the quark coefficient function. At the scale $Q^2 = 4 \text{ GeV}^2$ and in the \overline{MS} renormalization scheme at NLO, which are the scale and the scheme adopted in Refs. [36, 37], one gets $C_2^{NS} \simeq 1.01$ and $C_4^{NS} \simeq 1.15$.

The quark masses accessible in present lattice calculations are still relatively high and thus the extrapolation to the physical point is one of the open issues in lattice applications

Table 3: *Leading twist moments of the nonsinglet $p - n$ part of the F_2 structure function, $M_n^{p-n}(Q^2) = M_n^p(Q^2) - M_n^n(Q^2)$, together with statistical and systematic uncertainties.*

Q^2 [(GeV/c) ²]	$M_2^{p-n}(Q^2) \times 10^{-2}$	$M_4^{p-n}(Q^2) \times 10^{-2}$	$M_6^{p-n}(Q^2) \times 10^{-3}$	$M_8^{p-n}(Q^2) \times 10^{-3}$
1.025	6.1 ± 0.6 ± 1.0	1.74 ± 0.21 ± 0.12	9.39 ± 0.53 ± 0.12	7.78 ± 1.01 ± 1.66
1.075	6.0 ± 0.6 ± 1.0	1.67 ± 0.20 ± 0.11	8.56 ± 0.48 ± 0.11	6.48 ± 0.84 ± 1.38
1.125	6.0 ± 0.6 ± 1.0	1.62 ± 0.19 ± 0.11	7.91 ± 0.44 ± 0.11	5.58 ± 0.73 ± 1.19
1.175	5.9 ± 0.6 ± 1.0	1.57 ± 0.19 ± 0.11	7.38 ± 0.41 ± 0.11	4.92 ± 0.64 ± 1.05
1.225	5.9 ± 0.6 ± 1.0	1.52 ± 0.18 ± 0.10	6.94 ± 0.39 ± 0.10	4.42 ± 0.57 ± 0.94
1.275	5.8 ± 0.6 ± 1.0	1.48 ± 0.18 ± 0.10	6.57 ± 0.37 ± 0.10	4.03 ± 0.52 ± 0.86
1.325	5.8 ± 0.6 ± 1.0	1.45 ± 0.17 ± 0.10	6.25 ± 0.35 ± 0.10	3.71 ± 0.48 ± 0.79
1.375	5.8 ± 0.6 ± 1.0	1.42 ± 0.17 ± 0.10	5.98 ± 0.34 ± 0.10	3.45 ± 0.45 ± 0.74
1.425	5.7 ± 0.6 ± 1.0	1.39 ± 0.17 ± 0.09	5.74 ± 0.32 ± 0.09	3.23 ± 0.42 ± 0.69
1.475	5.7 ± 0.6 ± 1.0	1.36 ± 0.16 ± 0.09	5.53 ± 0.31 ± 0.09	3.04 ± 0.40 ± 0.65
1.525	5.7 ± 0.6 ± 1.0	1.34 ± 0.16 ± 0.09	5.35 ± 0.30 ± 0.09	2.88 ± 0.37 ± 0.62
1.575	5.7 ± 0.6 ± 0.9	1.31 ± 0.16 ± 0.09	5.18 ± 0.29 ± 0.09	2.75 ± 0.36 ± 0.59
1.625	5.6 ± 0.6 ± 0.9	1.29 ± 0.16 ± 0.09	5.03 ± 0.28 ± 0.09	2.62 ± 0.34 ± 0.56
1.675	5.6 ± 0.6 ± 0.9	1.27 ± 0.15 ± 0.09	4.89 ± 0.27 ± 0.09	2.52 ± 0.33 ± 0.54
1.725	5.6 ± 0.6 ± 0.9	1.26 ± 0.15 ± 0.08	4.77 ± 0.27 ± 0.08	2.42 ± 0.31 ± 0.52
1.775	5.6 ± 0.6 ± 0.9	1.24 ± 0.15 ± 0.08	4.65 ± 0.26 ± 0.08	2.33 ± 0.30 ± 0.50
1.825	5.5 ± 0.6 ± 0.9	1.22 ± 0.15 ± 0.08	4.54 ± 0.26 ± 0.08	2.25 ± 0.29 ± 0.48
1.875	5.5 ± 0.6 ± 0.9	1.21 ± 0.14 ± 0.08	4.45 ± 0.25 ± 0.08	2.18 ± 0.28 ± 0.47
1.925	5.5 ± 0.6 ± 0.9	1.19 ± 0.14 ± 0.08	4.36 ± 0.24 ± 0.08	2.12 ± 0.28 ± 0.45
1.975	5.5 ± 0.6 ± 0.9	1.18 ± 0.14 ± 0.08	4.27 ± 0.24 ± 0.08	2.06 ± 0.27 ± 0.44
2.025	5.4 ± 0.6 ± 0.9	1.17 ± 0.14 ± 0.08	4.19 ± 0.24 ± 0.08	2.00 ± 0.26 ± 0.43
2.075	5.4 ± 0.6 ± 0.9	1.16 ± 0.14 ± 0.08	4.12 ± 0.23 ± 0.08	1.95 ± 0.25 ± 0.42
2.125	5.4 ± 0.6 ± 0.9	1.15 ± 0.14 ± 0.08	4.05 ± 0.23 ± 0.08	1.91 ± 0.25 ± 0.41
2.175	5.4 ± 0.6 ± 0.9	1.13 ± 0.14 ± 0.08	3.99 ± 0.22 ± 0.08	1.86 ± 0.24 ± 0.40
2.225	5.4 ± 0.6 ± 0.9	1.12 ± 0.13 ± 0.08	3.93 ± 0.22 ± 0.08	1.82 ± 0.24 ± 0.39
2.275	5.4 ± 0.6 ± 0.9	1.11 ± 0.13 ± 0.07	3.87 ± 0.22 ± 0.07	1.79 ± 0.23 ± 0.38
2.325	5.3 ± 0.6 ± 0.9	1.11 ± 0.13 ± 0.07	3.82 ± 0.21 ± 0.07	1.76 ± 0.23 ± 0.38
2.375	5.3 ± 0.6 ± 0.9	1.10 ± 0.13 ± 0.07	3.78 ± 0.21 ± 0.07	1.73 ± 0.23 ± 0.37
2.425	5.3 ± 0.6 ± 0.9	1.09 ± 0.13 ± 0.07	3.74 ± 0.21 ± 0.07	1.70 ± 0.22 ± 0.36
2.475	5.3 ± 0.6 ± 0.9	1.08 ± 0.13 ± 0.07	3.70 ± 0.21 ± 0.07	1.68 ± 0.22 ± 0.36
2.525	5.3 ± 0.6 ± 0.9	1.08 ± 0.13 ± 0.07	3.66 ± 0.21 ± 0.07	1.66 ± 0.22 ± 0.35
2.575	5.3 ± 0.6 ± 0.9	1.07 ± 0.13 ± 0.07	3.62 ± 0.20 ± 0.07	1.63 ± 0.21 ± 0.35
2.625	5.3 ± 0.6 ± 0.9	1.06 ± 0.13 ± 0.07	3.58 ± 0.20 ± 0.07	1.61 ± 0.21 ± 0.34
2.675	5.3 ± 0.6 ± 0.9	1.06 ± 0.13 ± 0.07	3.55 ± 0.20 ± 0.07	1.59 ± 0.21 ± 0.34
2.725	5.2 ± 0.6 ± 0.9	1.05 ± 0.13 ± 0.07	3.52 ± 0.20 ± 0.07	1.57 ± 0.20 ± 0.33
2.775	5.2 ± 0.6 ± 0.9	1.04 ± 0.13 ± 0.07	3.48 ± 0.20 ± 0.07	1.55 ± 0.20 ± 0.33
2.825	5.2 ± 0.6 ± 0.9	1.04 ± 0.12 ± 0.07	3.45 ± 0.19 ± 0.07	1.53 ± 0.20 ± 0.33
2.875	5.2 ± 0.6 ± 0.9	1.03 ± 0.12 ± 0.07	3.42 ± 0.19 ± 0.07	1.51 ± 0.20 ± 0.32
2.925	5.2 ± 0.6 ± 0.9	1.03 ± 0.12 ± 0.07	3.40 ± 0.19 ± 0.07	1.50 ± 0.19 ± 0.32
2.975	5.2 ± 0.6 ± 0.9	1.02 ± 0.12 ± 0.07	3.37 ± 0.19 ± 0.07	1.48 ± 0.19 ± 0.32
3.025	5.2 ± 0.5 ± 0.9	1.02 ± 0.12 ± 0.07	3.34 ± 0.19 ± 0.07	1.47 ± 0.19 ± 0.31
3.075	5.2 ± 0.5 ± 0.9	1.01 ± 0.12 ± 0.07	3.32 ± 0.19 ± 0.07	1.45 ± 0.19 ± 0.31
3.125	5.2 ± 0.5 ± 0.9	1.01 ± 0.12 ± 0.07	3.29 ± 0.18 ± 0.07	1.44 ± 0.19 ± 0.31
3.175	5.1 ± 0.5 ± 0.9	1.00 ± 0.12 ± 0.07	3.27 ± 0.18 ± 0.07	1.42 ± 0.18 ± 0.30
3.225	5.1 ± 0.5 ± 0.9	1.00 ± 0.12 ± 0.07	3.24 ± 0.18 ± 0.07	1.41 ± 0.18 ± 0.30
3.275	5.1 ± 0.5 ± 0.9	0.99 ± 0.12 ± 0.07	3.22 ± 0.18 ± 0.07	1.40 ± 0.18 ± 0.30
3.325	5.1 ± 0.5 ± 0.9	0.99 ± 0.12 ± 0.07	3.20 ± 0.18 ± 0.07	1.38 ± 0.18 ± 0.29
3.375	5.1 ± 0.5 ± 0.8	0.98 ± 0.12 ± 0.07	3.18 ± 0.18 ± 0.07	1.37 ± 0.18 ± 0.29
3.425	5.1 ± 0.5 ± 0.8	0.98 ± 0.12 ± 0.07	3.16 ± 0.18 ± 0.07	1.36 ± 0.18 ± 0.29
3.475	5.1 ± 0.5 ± 0.8	0.98 ± 0.12 ± 0.07	3.14 ± 0.18 ± 0.07	1.35 ± 0.18 ± 0.29
3.525	5.1 ± 0.5 ± 0.8	0.97 ± 0.12 ± 0.07	3.12 ± 0.17 ± 0.07	1.34 ± 0.17 ± 0.28
3.575	5.1 ± 0.5 ± 0.8	0.97 ± 0.12 ± 0.07	3.10 ± 0.17 ± 0.07	1.32 ± 0.17 ± 0.28
3.625	5.1 ± 0.5 ± 0.8	0.96 ± 0.12 ± 0.06	3.08 ± 0.17 ± 0.06	1.31 ± 0.17 ± 0.28
3.675	5.1 ± 0.5 ± 0.8	0.96 ± 0.11 ± 0.06	3.06 ± 0.17 ± 0.06	1.30 ± 0.17 ± 0.28
3.725	5.1 ± 0.5 ± 0.8	0.96 ± 0.11 ± 0.06	3.04 ± 0.17 ± 0.06	1.29 ± 0.17 ± 0.28
3.775	5.0 ± 0.5 ± 0.8	0.95 ± 0.11 ± 0.06	3.03 ± 0.17 ± 0.06	1.28 ± 0.17 ± 0.27
3.825	5.0 ± 0.5 ± 0.8	0.95 ± 0.11 ± 0.06	3.01 ± 0.17 ± 0.06	1.28 ± 0.17 ± 0.27

Q^2 [(GeV/c) ²]	$M_2^{p-n}(Q^2) \times 10^{-2}$	$M_4^{p-n}(Q^2) \times 10^{-2}$	$M_6^{p-n}(Q^2) \times 10^{-3}$	$M_8^{p-n}(Q^2) \times 10^{-3}$
3.875	5.0 ± 0.5 ± 0.8	0.95 ± 0.11 ± 0.06	2.99 ± 0.17 ± 0.06	1.27 ± 0.16 ± 0.27
3.925	5.0 ± 0.5 ± 0.8	0.94 ± 0.11 ± 0.06	2.98 ± 0.17 ± 0.06	1.26 ± 0.16 ± 0.27
3.975	5.0 ± 0.5 ± 0.8	0.94 ± 0.11 ± 0.06	2.96 ± 0.17 ± 0.06	1.25 ± 0.16 ± 0.27
4.025	5.0 ± 0.5 ± 0.8	0.94 ± 0.11 ± 0.06	2.95 ± 0.17 ± 0.06	1.24 ± 0.16 ± 0.26
4.075	5.0 ± 0.5 ± 0.8	0.93 ± 0.11 ± 0.06	2.93 ± 0.16 ± 0.06	1.23 ± 0.16 ± 0.26
4.125	5.0 ± 0.5 ± 0.8	0.93 ± 0.11 ± 0.06	2.92 ± 0.16 ± 0.06	1.22 ± 0.16 ± 0.26
4.175	5.0 ± 0.5 ± 0.8	0.93 ± 0.11 ± 0.06	2.90 ± 0.16 ± 0.06	1.22 ± 0.16 ± 0.26
4.225	5.0 ± 0.5 ± 0.8	0.92 ± 0.11 ± 0.06	2.89 ± 0.16 ± 0.06	1.21 ± 0.16 ± 0.26
4.275	5.0 ± 0.5 ± 0.8	0.92 ± 0.11 ± 0.06	2.87 ± 0.16 ± 0.06	1.20 ± 0.16 ± 0.26
4.325	5.0 ± 0.5 ± 0.8	0.92 ± 0.11 ± 0.06	2.86 ± 0.16 ± 0.06	1.19 ± 0.16 ± 0.25
4.375	5.0 ± 0.5 ± 0.8	0.92 ± 0.11 ± 0.06	2.85 ± 0.16 ± 0.06	1.19 ± 0.15 ± 0.25
4.425	5.0 ± 0.5 ± 0.8	0.91 ± 0.11 ± 0.06	2.84 ± 0.16 ± 0.06	1.18 ± 0.15 ± 0.25
4.475	5.0 ± 0.5 ± 0.8	0.91 ± 0.11 ± 0.06	2.82 ± 0.16 ± 0.06	1.17 ± 0.15 ± 0.25
4.525	4.9 ± 0.5 ± 0.8	0.91 ± 0.11 ± 0.06	2.81 ± 0.16 ± 0.06	1.17 ± 0.15 ± 0.25
4.575	4.9 ± 0.5 ± 0.8	0.91 ± 0.11 ± 0.06	2.80 ± 0.16 ± 0.06	1.16 ± 0.15 ± 0.25
4.625	4.9 ± 0.5 ± 0.8	0.90 ± 0.11 ± 0.06	2.79 ± 0.16 ± 0.06	1.15 ± 0.15 ± 0.25
4.675	4.9 ± 0.5 ± 0.8	0.90 ± 0.11 ± 0.06	2.78 ± 0.16 ± 0.06	1.15 ± 0.15 ± 0.25
4.725	4.9 ± 0.5 ± 0.8	0.90 ± 0.11 ± 0.06	2.76 ± 0.16 ± 0.06	1.14 ± 0.15 ± 0.24
4.775	4.9 ± 0.5 ± 0.8	0.90 ± 0.11 ± 0.06	2.75 ± 0.15 ± 0.06	1.14 ± 0.15 ± 0.24
4.825	4.9 ± 0.5 ± 0.8	0.89 ± 0.11 ± 0.06	2.74 ± 0.15 ± 0.06	1.13 ± 0.15 ± 0.24
4.875	4.9 ± 0.5 ± 0.8	0.89 ± 0.11 ± 0.06	2.73 ± 0.15 ± 0.06	1.13 ± 0.15 ± 0.24
4.925	4.9 ± 0.5 ± 0.8	0.89 ± 0.11 ± 0.06	2.72 ± 0.15 ± 0.06	1.12 ± 0.15 ± 0.24
4.975	4.9 ± 0.5 ± 0.8	0.89 ± 0.11 ± 0.06	2.71 ± 0.15 ± 0.06	1.11 ± 0.14 ± 0.24
5.025	4.9 ± 0.5 ± 0.8	0.88 ± 0.11 ± 0.06	2.70 ± 0.15 ± 0.06	1.11 ± 0.14 ± 0.24
5.075	4.9 ± 0.5 ± 0.8	0.88 ± 0.11 ± 0.06	2.69 ± 0.15 ± 0.06	1.10 ± 0.14 ± 0.24
5.125	4.9 ± 0.5 ± 0.8	0.88 ± 0.11 ± 0.06	2.68 ± 0.15 ± 0.06	1.10 ± 0.14 ± 0.23
5.275	4.9 ± 0.5 ± 0.8	0.87 ± 0.10 ± 0.06	2.65 ± 0.15 ± 0.06	1.08 ± 0.14 ± 0.23
5.325	4.9 ± 0.5 ± 0.8	0.87 ± 0.10 ± 0.06	2.64 ± 0.15 ± 0.06	1.08 ± 0.14 ± 0.23
5.375	4.9 ± 0.5 ± 0.8	0.87 ± 0.10 ± 0.06	2.64 ± 0.15 ± 0.06	1.07 ± 0.14 ± 0.23
5.475	4.9 ± 0.5 ± 0.8	0.87 ± 0.10 ± 0.06	2.62 ± 0.15 ± 0.06	1.07 ± 0.14 ± 0.23
5.525	4.8 ± 0.5 ± 0.8	0.86 ± 0.10 ± 0.06	2.61 ± 0.15 ± 0.06	1.06 ± 0.14 ± 0.23
5.625	4.8 ± 0.5 ± 0.8	0.86 ± 0.10 ± 0.06	2.59 ± 0.15 ± 0.06	1.05 ± 0.14 ± 0.22
5.675	4.8 ± 0.5 ± 0.8	0.86 ± 0.10 ± 0.06	2.59 ± 0.15 ± 0.06	1.05 ± 0.14 ± 0.22
5.725	4.8 ± 0.5 ± 0.8	0.86 ± 0.10 ± 0.06	2.58 ± 0.14 ± 0.06	1.04 ± 0.14 ± 0.22
5.955	4.8 ± 0.5 ± 0.8	0.85 ± 0.10 ± 0.06	2.54 ± 0.14 ± 0.06	1.03 ± 0.13 ± 0.22
6.915	4.7 ± 0.5 ± 0.8	0.82 ± 0.10 ± 0.06	2.42 ± 0.14 ± 0.06	0.96 ± 0.12 ± 0.21
7.267	4.7 ± 0.5 ± 0.8	0.81 ± 0.10 ± 0.05	2.38 ± 0.13 ± 0.05	0.94 ± 0.12 ± 0.20
7.630	4.7 ± 0.5 ± 0.8	0.80 ± 0.10 ± 0.05	2.34 ± 0.13 ± 0.05	0.92 ± 0.12 ± 0.20
8.021	4.7 ± 0.5 ± 0.8	0.79 ± 0.10 ± 0.05	2.31 ± 0.13 ± 0.05	0.91 ± 0.12 ± 0.19
8.847	4.6 ± 0.5 ± 0.8	0.78 ± 0.09 ± 0.05	2.24 ± 0.13 ± 0.05	0.87 ± 0.11 ± 0.19
9.775	4.6 ± 0.5 ± 0.8	0.76 ± 0.09 ± 0.05	2.17 ± 0.12 ± 0.05	0.84 ± 0.11 ± 0.18
10.267	4.6 ± 0.5 ± 0.8	0.76 ± 0.09 ± 0.05	2.14 ± 0.12 ± 0.05	0.83 ± 0.11 ± 0.18
10.762	4.6 ± 0.5 ± 0.8	0.75 ± 0.09 ± 0.05	2.12 ± 0.12 ± 0.05	0.81 ± 0.11 ± 0.17
11.344	4.5 ± 0.5 ± 0.8	0.74 ± 0.09 ± 0.05	2.08 ± 0.12 ± 0.05	0.80 ± 0.10 ± 0.17
12.580	4.5 ± 0.5 ± 0.7	0.73 ± 0.09 ± 0.05	2.03 ± 0.11 ± 0.05	0.77 ± 0.10 ± 0.16
13.238	4.5 ± 0.5 ± 0.7	0.72 ± 0.09 ± 0.05	2.00 ± 0.11 ± 0.05	0.76 ± 0.10 ± 0.16
14.689	4.4 ± 0.5 ± 0.7	0.71 ± 0.08 ± 0.05	1.95 ± 0.11 ± 0.05	0.73 ± 0.09 ± 0.16
17.108	4.4 ± 0.5 ± 0.7	0.69 ± 0.08 ± 0.05	1.87 ± 0.11 ± 0.05	0.70 ± 0.09 ± 0.15
19.072	4.3 ± 0.5 ± 0.7	0.67 ± 0.08 ± 0.05	1.82 ± 0.10 ± 0.05	0.67 ± 0.09 ± 0.14
20.108	4.3 ± 0.5 ± 0.7	0.67 ± 0.08 ± 0.04	1.80 ± 0.10 ± 0.04	0.66 ± 0.09 ± 0.14
21.097	4.3 ± 0.5 ± 0.7	0.66 ± 0.08 ± 0.04	1.78 ± 0.10 ± 0.04	0.66 ± 0.09 ± 0.14
24.259	4.3 ± 0.5 ± 0.7	0.65 ± 0.08 ± 0.04	1.73 ± 0.10 ± 0.04	0.63 ± 0.08 ± 0.13
26.680	4.2 ± 0.5 ± 0.7	0.64 ± 0.08 ± 0.04	1.69 ± 0.09 ± 0.04	0.61 ± 0.08 ± 0.13
32.500	4.2 ± 0.4 ± 0.7	0.62 ± 0.07 ± 0.04	1.62 ± 0.09 ± 0.04	0.58 ± 0.08 ± 0.12
34.932	4.2 ± 0.4 ± 0.7	0.61 ± 0.07 ± 0.04	1.60 ± 0.09 ± 0.04	0.57 ± 0.07 ± 0.12
36.750	4.1 ± 0.4 ± 0.7	0.61 ± 0.07 ± 0.04	1.58 ± 0.09 ± 0.04	0.57 ± 0.07 ± 0.12
43.970	4.1 ± 0.4 ± 0.7	0.60 ± 0.07 ± 0.04	1.53 ± 0.09 ± 0.04	0.54 ± 0.07 ± 0.12
47.440	4.1 ± 0.4 ± 0.7	0.59 ± 0.07 ± 0.04	1.51 ± 0.08 ± 0.04	0.54 ± 0.07 ± 0.11
64.270	4.0 ± 0.4 ± 0.7	0.57 ± 0.07 ± 0.04	1.43 ± 0.08 ± 0.04	0.50 ± 0.06 ± 0.11
75.000	4.0 ± 0.4 ± 0.7	0.55 ± 0.07 ± 0.04	1.39 ± 0.08 ± 0.04	0.48 ± 0.06 ± 0.10
86.000	3.9 ± 0.4 ± 0.7	0.55 ± 0.07 ± 0.04	1.36 ± 0.08 ± 0.04	0.47 ± 0.06 ± 0.10
97.690	3.9 ± 0.4 ± 0.7	0.54 ± 0.06 ± 0.04	1.33 ± 0.07 ± 0.04	0.46 ± 0.06 ± 0.10

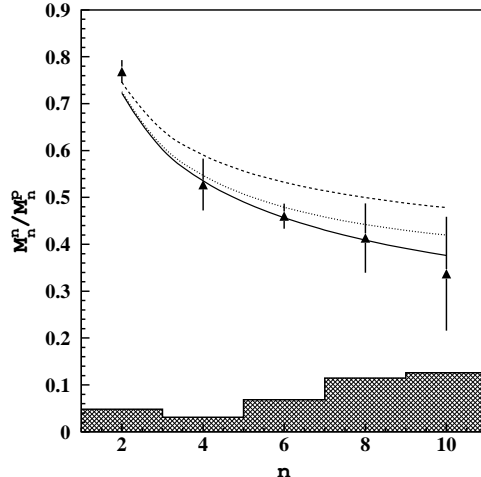


Figure 11: Ratio of the extracted neutron to proton leading twist moments (triangles) as a function of n , compared with the corresponding PDF parameterization of Ref. [29] (solid). The hatched area represents our systematic errors. The dashed and dotted curves correspond to the moment ratio evaluated after modifying the d -quark distribution according to Eq. (37) with $m = 1$ and $m = 4$, respectively.

to light hadron phenomenology. In Refs. [36, 37] the lattice data are extrapolated linearly in the quark masses up to the physical point, while in Ref. [38] the extrapolation includes the effects of meson loops and intermediate $\Delta(1232)$ resonance which are known to provide important non-analytic terms present in chiral perturbation theory.

Using Eq. (38) the results of Refs. [36, 37, 38] are translated in terms of nonsinglet $p - n$ moments, which are reported in Table 4 together with our corresponding results from Table 3. It can be seen that the results of Refs. [36, 37], which adopt a naive linear extrapolation in the quark masses up to the chiral point, are larger than our findings both at $n = 2$ and $n = 4$. Note that, by combining all the uncertainties, the deviations between our data and the lattice results of Refs. [36, 37] are $\approx 3.3\sigma$ at $n = 2$, but only $\approx 1.6\sigma$ at $n = 4$. The results of Ref. [38], which includes the effects of meson loops and intermediate $\Delta(1232)$ resonance in the chiral extrapolation, are in excellent agreement with our numbers for both $n = 2$ and $n = 4$. It should be mentioned that the role of finite volume effects at small quark masses still remains to be investigated.

4 Isospin dependence of the Higher Twist contribution

Once the leading twist is settled and checked, one can study the isospin dependence of the higher twist (HT) contribution. Previous studies were performed in x -space in Refs. [39, 40]. These analyses showed that in the region $x \leq 0.7$ HT terms are approximately the

Table 4: Comparison of the nonsinglet leading twist moments of the F_2 structure function given in Table 3 with the lattice predictions from Refs. [36, 37, 38] at the scale $Q^2 = 4 \text{ GeV}^2$.

n	This work	Ref. [36]	Ref. [37]	Ref. [38]
2	0.050 (5) (8)	0.091 (8)	0.082 (3)	0.059 (8)
4	0.0094 (11) (6)	0.030 (16)	0.023 (7)	0.009 (3)

same for the proton and the deuteron, while at larger x some isospin dependence was seen in Ref. [40], but not in Ref. [39] (although the experimental errors in Ref. [39] were much larger than the difference between the HTs in the proton and in the deuteron).

In the present paper we consider the total HT contribution in moment space, simply defined as the difference between the total and leading twist moments of F_2 ,

$$\text{HT}_n^N(Q^2) = M_n^{N(\text{tot})}(Q^2) - M_n^N(Q^2), \quad (39)$$

where the leading twist moment $M_n^N(Q^2)$ is defined as in Eq. (2).

Let us briefly recall that our approach is characterized by some relevant features which are essential for a reliable extraction of the HT contribution. In particular: (i) the target mass corrections are removed from the total moments through the use of the Nachtmann definition; (ii) effective HT anomalous dimensions are extracted phenomenologically; (iii) the effects of Sudakov logarithms are taken into account through Soft Gluon Resummation; and (iv) the running coupling constant $\alpha_s(M_Z^2)$ is consistently extracted from the proton moments at high Q^2 [41], giving the value $\alpha_s(M_Z^2) = 0.1188 \pm 0.0010_{\text{stat}} \pm 0.0014_{\text{syst}}$, which is consistent with the latest world average value $\alpha_s(M_Z^2) = 0.1187 \pm 0.0020$ [42]. As a result the total higher twist contribution $\text{HT}_n^N(Q^2)$ is extracted reliably and with good precision both for the proton and deuteron [5, 6] for $Q^2 \gtrsim 1 \text{ GeV}^2$.

In Fig. 12 the total HT term in the proton moments, $\text{HT}_n^p(Q^2)$, is compared with that in the deuteron, $\text{HT}_n^D(Q^2)$, after applying to the latter the same nuclear corrections used for the leading twist, namely \mathcal{F}_n^D of Eq. (14). Within the quoted uncertainties the higher twists appear to be the same in the proton and deuteron (per nucleon) moments. Assuming that possible additional nuclear effects are small with respect to the moment uncertainties (at least for $Q^2 \gtrsim 1 \text{ GeV}^2$), the total HT contribution appears to be isospin-independent. This means that for the isovector combination $p - n$ our total HT term is consistent with zero within the uncertainties.

Based on the above results we now speculate about two possible scenarios in which our findings can be interpreted:

1. isospin-independent $q - q$ correlations.
2. dominance of $u - d$ correlations with respect to $u - u$ and $d - d$ ones.

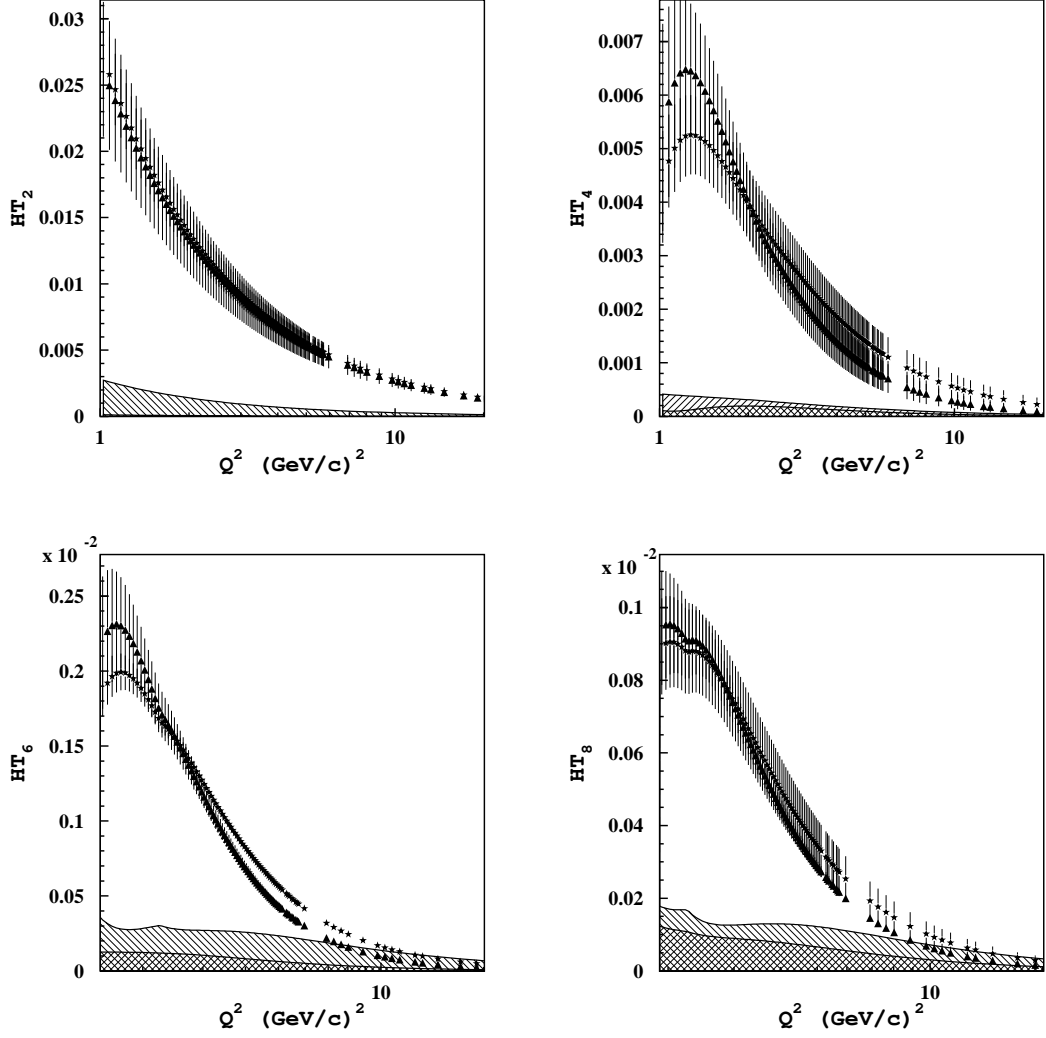


Figure 12: Total higher twist contribution to the moments with $n = 2, 4, 6, 8$ together with their statistical (bars) and systematic (left- and across-hatched areas) uncertainties: triangles show the higher twist contribution in the proton moments and the stars represent the same contribution in the deuteron moments corrected by the Fermi motion factor \mathcal{F}_n^D given in Eq. (14). The left- and cross-hatched areas refer to the case of proton and deuteron, respectively.

Assuming that HTs are dominated by coupling of the virtual boson with correlated qq pairs, the neutron to proton ratio of HTs is expected to be

$$\frac{HT^n}{HT^p} = \frac{2(ud)\frac{1}{9} + (dd)\frac{4}{9}}{2(ud)\frac{1}{9} + (uu)\frac{16}{9}} \quad (40)$$

If $q - q$ correlations are isospin-independent, the HT ratio (40) becomes equal to $1/3$, a value which is not supported by the present analysis.

The second scenario can be better understood in terms of a diquark model (see [43] and references therein), which represent a simple, natural way to account for the so-called lack of missing nucleon resonances. The correlation between two quarks in a 0^+ color antitriplet state is expected to be of particular importance [43, 44]. Indeed, such a configuration is very likely in the nucleon because the correlation between two quarks in a color antitriplet state forming a scalar, isoscalar diquark is as strong as the corresponding $\bar{q}q$ correlation in the pion, as it is known from both QCD sum rules [45] and instanton calculations [46]. The most dramatic effect of scalar, isoscalar diquark formation occurs in strangeness changing weak decays at low energies, leading to the explanation of the huge $\Delta I = 1/2$ enhancement present in these processes [47].

In the quark-diquark picture of the nucleon diquarks are expected to be spatially extended objects and therefore it is natural to consider that HT terms in lepton-nucleon DIS originate mainly from the elastic scattering of the virtual boson off diquarks, representing correlated pairs of quarks. Many applications of the quark-diquark model to nucleon observables indicate that scalar, isoscalar diquarks are more abundant and have a size smaller than the one of vector, isovector diquarks [43]. This means that $u - d$ correlations are expected to dominate over $u - u$ and $d - d$ ones, and therefore the HT ratio (40) becomes equal to 1, a value which is fully consistent with our findings. A clear-cut determination of the spin of the dominant $u - d$ diquark requires the simultaneous investigation of the HTs in the longitudinal channel.

Before closing this Section, we want to point out that, if HTs are isospin-independent, then the nuclear correction can be obtained directly from the ratio between higher twist contributions in the deuteron and proton moments. In Fig. 13 such a ratio is compared with the nuclear correction factor given by Eq. (14). The agreement is reasonable within the statistical and systematic error bars.

5 Conclusions and future directions

We have extracted the leading twist contribution to first few moments ($n = 2 - 10$) of the neutron structure function F_2 in the Q^2 range from 1 up to 100 GeV^2 , by combining proton and deuteron measurements over a huge range of kinematics. We have paid particular attention to the issue of nuclear effects in the deuteron, which are found to be increasingly important for the higher moments. The model dependence arising from our incomplete knowledge of the nuclear corrections, including the high-momentum tail of the deuteron wave function, as well as nucleon off-shell effects, were estimated and included in the systematic errors. From our analysis the following conclusions can be made:

- the extracted moments of the neutron structure function F_2 are consistent at large Q^2 with the predictions of several PDFs available in the literature;
- the ratio of neutron to proton structure functions is determined from the ratio of

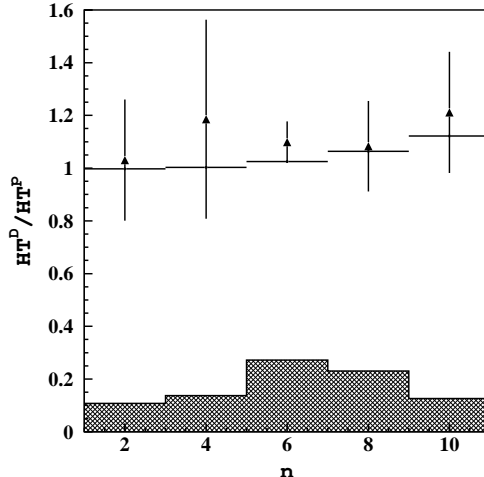


Figure 13: *Ratio of the deuteron to the proton higher twist contribution at $Q^2 = 3 \text{ GeV}^2$ with its statistical and systematic uncertainties represented by bars and hatched area, respectively. The solid curve represents the nuclear correction factor \mathcal{F}_n^D defined in Eq. (14).*

the corresponding moments up to $x \simeq 0.70$; we find $F_2^n/F_2^p(x = 0.70) = 0.34 \pm 0.12_{\text{stat}} \pm 0.13_{\text{syst}}$. Our results are consistent with the asymptotic limit $1/4$ at $x = 1$, which originates from the dominance of soft, non-perturbative physics at large x . Nevertheless the alternative limiting value of $3/7$, derived from helicity conservation arguments, is not excluded at all, but the possible enhancement of the d -quark distribution should be confined to the region $x \gtrsim 0.7$;

- the nonsinglet, isovector $p - n$ combination of the leading twist moments is constructed and compared with available lattice results. We have found that our data are larger than the lattice values of Refs. [36, 37], extrapolated linearly in the quark masses down to the physical point, by $\approx 3.3\sigma$ for the second moment, but only by $\approx 1.6\sigma$ in case of the fourth moment. Our results are in excellent agreement with those of Ref. [38], where the chiral extrapolation is performed taking into account the effects of non-analytic terms due to meson loops and intermediate $\Delta(1232)$ resonance;
- the total contribution of higher twists is found to be isospin independent, which implies that in the isovector combination $p - n$ the higher twists are consistent with zero within the uncertainties. The isospin independence is expected in a quark-diquark picture of the nucleon assuming the dominance of isoscalar $u - d$ diquarks.

The determination of the large- x behavior of the d -quark distribution in the nucleon is still one of the main unsolved problems in partonic physics. The use of deuteron

inclusive DIS data to extract the neutron to proton structure function ratio produces unavoidably a model dependence. The strategy used in this paper has its own practical limitations which are due to the increasing uncertainties of the nuclear corrections as the order of the moments considered increases. It appears that moments of order $n = 12$ may be still accessible by improving measurements of the structure function F_2 at large x . As we have shown, at $n = 12$ one can probe values of the Bjorken- x as large as 0.75, which represents therefore an upper limit.

Future directions for the experimental determination of the d -quark distribution at high x have been recently discussed in the literature [48, 49, 50, 51]. One of the strategies, which is currently under experimental investigation at Jefferson Lab [52], is the use of the tagged semi-inclusive process off the deuteron [48, 49], which requires the detection of a low momentum proton ($p \lesssim 150 \text{ MeV}/c$). An alternative method which has been discussed, tries to exploit the mirror symmetry of $A = 3$ nuclei to reduce nuclear effects in the extraction of the F_2^n/F_2^p ratio [50, 51].

In the semi-inclusive deuteron method one can *tag* the momentum of the struck neutron by detecting the slow recoiling proton; in this way it is possible to select initial deuteron configurations in which the two nucleons are far apart, so that the struck nucleon can be considered as free and the uncertainties due to the low-momentum part of the deuteron wave function are minimal [48, 49]. The neutron structure function can then be extracted directly from the semi-inclusive deuteron cross section.

We want to point out that an important improvement of the *tagged* strategy may be achieved by adding the detection of slow recoiling neutrons. In this way the n/p structure function ratio can be directly obtained from the ratio of the corresponding semi-inclusive cross sections. Most of the nuclear corrections, e.g. Fermi motion, off-shellness and FSIs, are expected to largely cancel out in the ratio [48, 49]. Thus, from the measurements of both semi-inclusive processes $D(e, e'p)X$ and $D(e, e'n)X$ the shape of the d -quark distribution may be experimentally investigated up to and hopefully beyond $x \approx 0.75$.

Acknowledgements

The work of W.M. was supported by the U.S. Department of Energy contract DE-AC05-84ER40150, under which the Southeastern Universities Research Association (SURA) operates the Thomas Jefferson National Accelerator Facility (Jefferson Lab). The work of S.K. was partially supported by the Russian Foundation for Basic Research grant 03-02-17177 and INTAS project 03-51-4007.

References

- [1] B. Badelek and J. Kwiecinski, *Nucl. Phys.* **B370**, 278 (1992); *Phys. Rev.* **D50**, 4 (1994). V. R. Zoller, *Z. Phys.* **C54**, 425 (1992). V. Barone, M. Genovese, N. N. Nikolaev, E. Predazzi and B. G. Zakharov, *Phys. Lett.* **B321**, 137 (1994).

- [2] G. Piller, W. Ratzka and W. Weise, *Z. Phys.* **A352**, 427 (1995) [arXiv:hep-ph/9504407]. G. Piller and W. Weise, *Phys. Rept.* **330**, 1 (2000) [arXiv:hep-ph/9908230].
- [3] W. Melnitchouk and A.W. Thomas, *Phys. Rev.* **D47**, 3783 (1993).
- [4] S. A. Kulagin, G. Piller and W. Weise, *Phys. Rev.* **C50**, 1154 (1994) [arXiv:nucl-th/9402015].
- [5] M. Osipenko *et al.*, *Phys. Rev.* **D67**, 092001 (2003); CLAS-NOTE-2003-001 (September 2003) [arXiv:hep-ex/0309052]
- [6] M. Osipenko *et al.*, arXiv:hep-ex/0506004; CLAS-NOTE-2005-013 (July 2005) [arXiv:hep-ex/0507098]
- [7] G.B. West, *Phys. Lett.* **B37**, 509 (1971).
- [8] R.L. Jaffe, in *Relativistic Dynamics and Quark-Nuclear Physics*, ed. by M.B. Johnson and A. Pickleseimer, Wiley (New York, 1985), pp. 1-82.
- [9] R.P. Bickerstaff and A.W. Thomas, *J. Phys.* **G15**, 1523 (1989). L.L. Frankfurt and M.I. Strikman, *Phys. Lett.* **B64**, 433 (1976); **76B**, 333 (1978). S.V. Akulinichev, S.A. Kulagin and G.M. Vagrado, *Phys. Lett.* **B158**, 485 (1985). S.A. Kulagin, *Nucl. Phys.* **A500**, 653 (1989).
- [10] J. A. Tjon and M. J. Zuilhof, *Phys. Lett.* **B84**, 31 (1979). E. Hummel and J. A. Tjon, *Phys. Rev. Lett.* **63**, 1788 (1989); *Phys. Rev.* **C49**, 21 (1994) [arXiv:nucl-th/9309004].
- [11] W. W. Buck and F. Gross, *Phys. Rev.* **D20**, 2361 (1979).
- [12] F. Gross, J. W. Van Orden and K. Holinde, *Phys. Rev.* **C45**, 2094 (1992).
- [13] W. Melnitchouk, A. W. Schreiber and A. W. Thomas, *Phys. Rev.* **D49**, 1183 (1994) [arXiv:nucl-th/9311008].
- [14] W. Melnitchouk, A.W. Schreiber and A.W. Thomas, *Phys. Lett.* **B335**, 11 (1994).
- [15] W. Melnitchouk and A.W. Thomas, *Acta Phys. Polon.* **B27**, 1407 (1996).
- [16] L. L. Frankfurt and M. I. Strikman, *Phys. Rept.* **76**, 215 (1981).
- [17] J. Carbonell, B. Desplanques, V. A. Karmanov and J. F. Mathiot, *Phys. Rept.* **300**, 215 (1998) [arXiv:nucl-th/9804029]; V. A. Karmanov, *Nucl. Phys.* **A362**, 331 (1981).
- [18] M. Lacombe *et al.*, *Phys. Rev.* **C21**, 861 (1980).
- [19] R. Machleidt, K. Holinde and C. Elster, *Phys. Rept.* **149**, 1 (1987).

- [20] R. Machleidt, F. Sammarruca and Y. Song, *Phys. Rev.* **C53**, R1483 (1996).
- [21] V.G.J. Stoks *et al.*, *Phys. Rev.* **C49**, 2950 (1994).
- [22] R.B. Wiringa, V.G.J. Stoks and R. Schiavilla, *Phys. Rev.* **C51**, 38 (1995).
- [23] O. Nachtmann, *Nucl. Phys.* **B63**, 237 (1973).
- [24] C. Ciofi degli Atti and S. Simula, *Phys. Rev.* **C53**, 1689 (1996); *Phys. Lett.* **B325**, 276 (1994).
- [25] S. A. Kulagin and R. Petti, arXiv:hep-ph/0412425.
- [26] L.P. Kaptari and A.Yu. Umnikov, *Phys. Lett.* **B272**, 359 (1991).
- [27] M. Glück, E. Reya and A. Vogt: *Eur. Phys. J.* **C5** (1998) 461 [arXiv:hep-ph/9806404]
- [28] A.D. Martin, R.G. Roberts, W.J. Stirling and R.S. Thorne: *Eur. Phys. J.* **C39** (2005) 155 [arXiv:hep-ph/0411040]
- [29] J. Pumplin, D.R. Stump, J. Huston, H.L. Lai, D. Nadolsky and W.K. Tung: *JHEP* **07** (2002) 012 [arXiv:hep-ph/0201195]
- [30] S. Alekhin: *Phys. Rev.* **D68** (2003) 014002 [hep-ph/0211096]. See also A. Vogt, S. Moch and J.A.M. Vermaseren: *Nucl. Phys.* **B691** (2004) 129 [arXiv:hep-ph/0404111]
- [31] S. Simula, *Phys. Lett.* **B493**, 325 (2000).
- [32] G. P. Lepage and S. J. Brodsky, *Phys. Rev. D* **22**, 2157 (1980).
- [33] R.P. Feynman, *Photon Hadron Interactions*, Benjamin, New York, 1972.
- [34] G.R. Farrar and D.R. Jackson, *Phys. Rev. Lett.* **35**, 1416 (1975). S.J. Brodsky and G.R. Farrar, *Phys. Rev.* **D11**, 229 (1975).
- [35] U.K. Yang and A. Bodek, *Phys. Rev. Lett.* **82**, 2467 (1999).
- [36] D. Dolgov *et al.* (LHPC and SESAM Collaborations), *Phys. Rev.* **D66**, 034506 (2002).
- [37] M. Goeckeler *et al.* (QCDSF Collaboration), hep-ph/0410187.
- [38] W. Detmold *et al.*, *Phys. Rev. Lett.* **87**, 172001 (2001). W. Detmold, W. Melnitchouk and A.W. Thomas, *Phys. Rev.* **D66**, 054501 (2002).
- [39] M. Virchaux and A. Milsztajn, *Phys. Lett.* **B274**, 221 (1992).
- [40] S.I. Alekhin, S.A. Kulagin and S. Liuti, *Phys. Rev.* **D69**, 114009 (2004).

- [41] S. Simula and M. Osipenko, *Nucl. Phys.* **B675**, 289 (2003).
- [42] S. Eidelman et al., *Phys. Lett.* **B592**, 1 (2004).
- [43] M. Anselmino *et al.*, *Rev. Mod. Phys.* **65**, 1199 (1993). P. Kroll, *Few Body Syst. Suppl.* **11**, 255 (1999).
- [44] R. Jaffe, F. Wilczek, *Phys. Rev. Lett.* **91**, 232003 (2003).
- [45] G. Dosch, M. Jamin, B. Stech, *Z. Phys.* **C42**, 167 (1989); M. Jamin, M. Neubert, *Phys. Lett.* **B238**, 387 (1990).
- [46] E. V. Shuryak, *Nucl. Phys.* **B203**, 93 (1982). T. Schäfer, E.V. Shuryak, *Mod. Phys.* **70**, 323 (1998). M. Cristoforetti *et al.*, *Phys. Rev.* **D71**, 114010 (2005).
- [47] B. Stech, *Phys. Rev.* **D36**, 975 (1987). M. Neubert, B. Stech, *Phys. Rev.* **D44**, 775 (1991). B. Stech, Q.P. Xu, *Z. Phys.* **C49**, 491 (1991). B. Stech, *Mod. Phys. Lett.* **A6**, 3113 (1991). M. Cristoforetti *et al.*, *Phys. Rev.* **D70**, 054016 (2004).
- [48] W. Melnitchouk, M. Sargsian and M.I. Strikman, *Z. Phys.* **A359**, 99 (1997); see also arXiv:nucl-th/9609048.
- [49] S. Simula, *Phys. Lett.* **B387**, 245 (1996); *Nucl. Phys.* **A631**, 602c (1997); see also arXiv:nucl-th/9608053.
- [50] I.R. Afnan *et al.*, *Phys. Lett.* **B493**, 36 (2000). E. Pace *et al.*, *Phys. Rev.* **C64**, 055203 (2001). I.R. Afnan *et al.*, *Phys. Rev.* **C68**, 035201 (2003).
- [51] M.M. Sargsian, S. Simula and M.I. Strikman, *Phys. Rev.* **C66**, 024001 (2002).
- [52] Bound Nucleon Structure Function (BoNuS) Collaboration at Jefferson Lab, Hall-B experiment E-03-012, S. Kuhn, C. Keppel and W. Melnitchouk spokespersons.